Molecular Neurobiology (2019) 56:5671–5688
https://doi.org/10.1007/s12035-018-1436-7

Steroid-Enriched Fraction of *Achyranthes bidentata* Protects Amyloid β Peptide 1–40-Induced Cognitive Dysfunction and Neuroinflammation in Rats

Li-Wei Lin[1] · Fan-Hsuan Tsai[1] · Wan-Cheng Lan[2] · Yih-Dih Cheng[3] · Sheng-Chi Lee[4] · Chi-Rei Wu[2]

Received: 9 April 2018 / Accepted: 20 November 2018 / Published online: 21 January 2019

Abstract

The roots of *Achyranthes bidentata* Blume (AB) is commonly used in the treatment of osteoporosis and dementia in traditional Chinese medicine. Pharmacological reports evidenced that AB possessed anti-osteoarthritis effects. However, there is little literature about the anti-dementia activities of AB. The present study was designed to prepare steroid-enriched fraction of AB (ABS) and investigate whether ABS can protect from cognitive dysfunction and neuroinflammation against Aβ 1–40-induced Alzheimer's disease (AD) model in rats. ABS only contained 135.11 ± 4.28 mg of ecdysterone per gram. ABS (50 mg/kg) reversed the dysfunction of exploratory activity and memory function on plus-maze and Morris water maze caused by Aβ 1–40 in rats. ABS (50 mg/kg) also decreased amyloid deposition, neurofibrillary tangle, neural damage, activated astrocyte, and microglial caused by Aβ 1–40. Furthermore, ABS reversed the phenomenon of neural oxidative damage and neuroinflammation, including the higher levels of MDA and cytokines, and the lower activities of antioxidant enzymes and GSH levels caused by Aβ 1–40 in rat cortex and hippocampus. Finally, ABS restored the activation of ERK pathway and decreased NF-κB phosphorylation and translocation altered by Aβ 1–40. ABS alone (50 mg/kg) promoted cognitive function, activated brain antioxidant defense system, and decreased brain TNF-α levels in sham group. Therefore, ABS has the cognition-promoting and antidementia potential. Steroids especial ecdysterone are major active components of AB. The action mechanism is due to decreasing oxidative stress and neuroinflammation through modulating ERK pathway, NF-κB phosphorylation, and translocation in Aβ 1–40-induced AD rat model.

Keywords *Achyranthes bidentata* · Ecdysterone · Aβ 1–40 · Oxidative stress · Neuroinflammation · ERK/NF-κB pathway · Hippocampus

Introduction

Alzheimer's disease (AD), a highly prevalent progressive neurodegenerative disorder, is mainly characterized by cognitive deficits and major neuropathological symptom such as extracellular senile plaque and intracellular and neurofibrillary tangle (NFT) [1, 2]. Amyloid β peptide (Aβ) has long been reported as a key component of extracellular senile plaque.

Li-Wei Lin and Fan-Hsuan Tsai contributed equally to this work.

Electronic supplementary material The online version of this article (https://doi.org/10.1007/s12035-018-1436-7) contains supplementary material, which is available to authorized users.

✉ Sheng-Chi Lee
osclee.tw@msa.hinet.net

✉ Chi-Rei Wu
crw@mail.cmu.edu.tw

Li-Wei Lin
lwlin@isu.edu.tw

Fan-Hsuan Tsai
asura0734@isu.edu.tw

[1] School of Chinese Medicines for Post-Baccalaureate, I-Shou University, Kaohsiung 82445, Taiwan

[2] Department of Chinese Pharmaceutical Sciences and Chinese Medicine Resources, China Medical University, Taichung 40402, Taiwan

[3] Department of Pharmacy, China Medical University Hospital, Taichung 40402, Taiwan

[4] Pintung Branch, Kaohsiung Veterans General Hospital, Pitung 91245, Taiwan

When Aβ oligomer is aggregated and deposited in the brain especial entorhinal cortex and hippocampus, it causes neuronal loss and cognitive deficits [3, 4]. High Aβ levels in the brain causes two mainly pathological consequences which are oxidative stress and neuroinflammation. Aβ plaques interfered with electron transport chain and thus produced reactive oxygen species (ROS) and caused intracellular oxidative stress. Furthermore, ROS activated many downstream signaling molecules, such as mitogen-activated protein kinases (MAPKs) that induce nuclear translocation of nuclear factor kappa-light-chain-enhancer of activated B cells (NF-κB) and the expression of pro-inflammatory genes such as interleukin-1β (IL-1β), IL-6, and tumor necrosis factor-α (TNF-α) [5–7]. Thus, the reduction of Aβ deposition, oxidative stress, and neuroinflammation are promising targets for AD treatment [2, 8]. Recent researchers have suggested that anti-inflammatory agents, antioxidants, and intracellular signaling modulators were beneficial for AD patients [8–10].

The roots of *Achyranthes bidentata* Blume (AB, Huai Niu-Xi in Chinese name), belonging to Amaranthaceae, are commonly used in the treatment of osteoporosis and dementia in the traditional Chinese medicine [11]. Recent reports have evidenced that AB extracts possessed anti-osteoarthritis and anti-inflammatory effects [12, 13]. Phytochemical screening revealed the major constituents of AB extracts in anti-osteoarthritis and anti-inflammatory effects were saponins, steroids and polysaccharides, especial oleanolic acid, ursolic acid, and ecdysterone [11]. As to the treatment in dementia by traditional Chinese physicians, the previous study only reported that ethanolic extract of AB prevented Aβ 1-42 aggregation [14]. The series reports of Ding et al. indicated that the aqueous extract of AB protected from apoptosis and neuroinflammation against MPP^+ in SH-SY5Y cells, primary dopaminergic neurons, and in MPTP-induced Parkinson's disease (PD) model. Ding et al. indicated that the major constituents of AB extracts in neuroprotective effects are polypeptides [15]. Due to that there is little investigation in the neuroprotective effects of AB on dementia and AD, the present study was designed to prepare AB and the steroid-enriched fraction of AB (ABS) and investigate whether AB or ABS could protect from cognitive dysfunction and neuroinflammation against Aβ 1–40-induced AD model in rats.

Materials and Methods

Extraction and Fractionation of Plant Material

Roots of *Achyranthes bidentata* (1.5 kg) were purchased from Chinese Medicine Pharmacy in Taiwan and authenticated by Dr. Chi-Rei Wu from Department of Chinese Pharmaceutical Sciences and Chinese Medicine Resources. AB were pulverized, soaked for 12 h with 16 L 80% ethanol, and extracted for three times for 2 h at 80 °C. The ethanolic solution was filtered and dried using a rotary evaporator under reduced pressure. The resulting ethanol extract (AB, 84 g, 5.6%) was suspended in water, and then successively partitioned with petroleum ether and water-saturated *n*-butanol. The *n*-butanolic fraction was dried using freezer and steroid-enriched fraction of AB (ABS) was obtained (12.9 g, 0.86%). The used doses of AB (100, 500 mg/kg body weight) and ABS (10, 50 mg/kg body weight) were based on the clinical therapeutic doses (5–12 g/day) of AB described in Taiwan Herbal Pharmacopeia or Pharmacopeia of People's Republic of China [16, 17] and the used dosage (4–8 mg/kg) of ecdysterone in Aβ 25–35 intrahippocampal injection model [18] and dissolved with 0.5% carboxymethylcellulose.

Determination of Ecdysterone, Oleanolic Acid, and Ursolic Acid by High-Performance Liquid Chromatography

ABS was dissolved in methanol and then filtered using a 0.22-μm filter. Ecdysterone, oleanolic acid, and ursolic acid were purchased from Extrasynthese (Lyon Nord, GENAY, France). Stock solutions of standards including ecdysterone, oleanolic acid, and ursolic acid were also prepared in methanol to the final concentration 1 mg/mL. All standard and sample solutions were injected into 10 μL in triplicate. The Shimadzu VP series high-performance liquid chromatography (HPLC) and Shimadzu Class-VP™ chromatography data systems were used. A Supelco Discovery® C18 (150 × 4.6 mm, 5 μm) column (Sigma-Aldrich Co., St Louis, MO, USA) was used. The separating conditions including the mobile phase and gradient program condition were modified from the description by Zhang et al. [19]. All chromatographic operations were performed at 25 °C. The chromatographic peaks of ecdysterone, oleanolic acid, and ursolic acid were confirmed by comparing their retention times and UV spectra.

Animals

Male Sprague-Dawley rats (300–350 g) were obtained from BioLASCO Taiwan Co., Ltd. They were housed in groups of four, chosen at random, in wire-mesh cages (39 cm × 26 cm × 21 cm) in a temperature- (23 ± 1 °C) and humidity (60%)-regulated environment with a 12 h–12 h light/dark cycle (light phase: 08:00 to 20:00). The Institutional Animal Care and Use Committee of I-Shou University approved the experimental protocol (IACUC-ISU-9905), and the animals were cared according to the Guiding Principles for the Care and Use of Laboratory Animals. After 1 week of acclimatization, the rats were used in the experiments that are described below.

Intracisternal Aβ 1–40 Injection Model

An Aβ 1–40-injected rat model was developed by injecting Aβ 1–40 into the cerebral ventricle via a microsyringe pump (KD Scientific Inc., Holliston, MA, USA). Briefly, Aβ 1–40-injected rats were anesthetized with phenobarbital (45 mg/kg, i.p.) and placed in a David Kopf stereotaxic instrument. Each Aβ 1–40-injected rat was injected in the left cerebral ventricle (AP-1.5, ML + 0.9, V-3.6 from Bregma) using a 10-μL microsyringe (Hamilton, Reno, NV, USA) fitted with 30-gauge stainless steel needle with a rate of 1 μL/min, and the injection needle was left in place for another 1 min to allow diffusion and to avoid the reflux of the solution [20]. Aβ 1–40 (5 nmol/μL) was purchased from Anaspec Inc. (Fremont, CA, USA) and dissolved with 0.1 M PBS at pH 7.4, and aliquots were stored at − 20 °C. Aβ 1–40 in each aliquot were aggregated by incubation in sterile distilled water at 37 °C for 2 days. Sham rats treated with vehicle, AB (100, 500 mg/kg), ABS (10, 50 mg/kg) were performed as the above procedure of Aβ 1–40 injection but intracisternally injected with PBS to replace Aβ 1–40.

Experimental Design

The schedule of surgery, drug treatments, and behavioral measurements is shown in Fig. 1. On the day (day 1) after PBS or Aβ 1–40 injection, the rats were orally administered with vehicle, AB (100, 500 mg/kg), or ABS (10, 50 mg/kg). The behavioral measurements were carried out from day 8 to day 15 after PBS or Aβ 1–40 injection, in the order, locomotor and exploratory tests (day 8), elevated plus maze (day 9–10), and spatial performance test and probe test in Morris water maze (MWM) (day 11–15). On day 16 after PBS or Aβ 1–40 injection, the rats were sacrificed 1 h after their final treatment with vehicle or ABS (10, 50 mg/kg) to measure the activities of acetylcholinesterase (AChE) and antioxidant enzymes (superoxide dismutase (SOD), glutathione peroxide (GPx), glutathione reductase (GR), and catalase), and the levels of glutathione (GSH), malondialdehyde (MDA), and cytokines (IL-1β, IL-6, and TNF-α) in cortex and hippocampus.

Behavioral Tests

Locomotor and Exploratory Tests

Locomotor and exploratory tests were simultaneously performed with open-field task (Coulbourn Instruments L.L.C., Holliston, MA, PA, USA) on day 8 after Aβ 1–40 injection. Each rat was put into open-field apparatus whose nose poke floor has 16 circular holes (1.4 × 1.4 cm) and observed for 10 min to record the movement time, distance, and velocity (locomotor activity); the number of entries it made into the hole; and the time spent in the hole (exploratory activity) using TruScan software v 2.07 (Coulbourn Instruments L.L.C.) [21].

Elevated Plus-Maze

On days 9–10, the elevated plus-maze was performed. The plus maze consisted of two open arms (50 × 10 cm) and two enclosed arms (50 × 10 × 40 cm) extending from a central platform (10 × 10 cm). The arms were elevated to a 50-cm height above the floor. On the acquisition session, each rat was placed at the distal end of the open arm facing away from

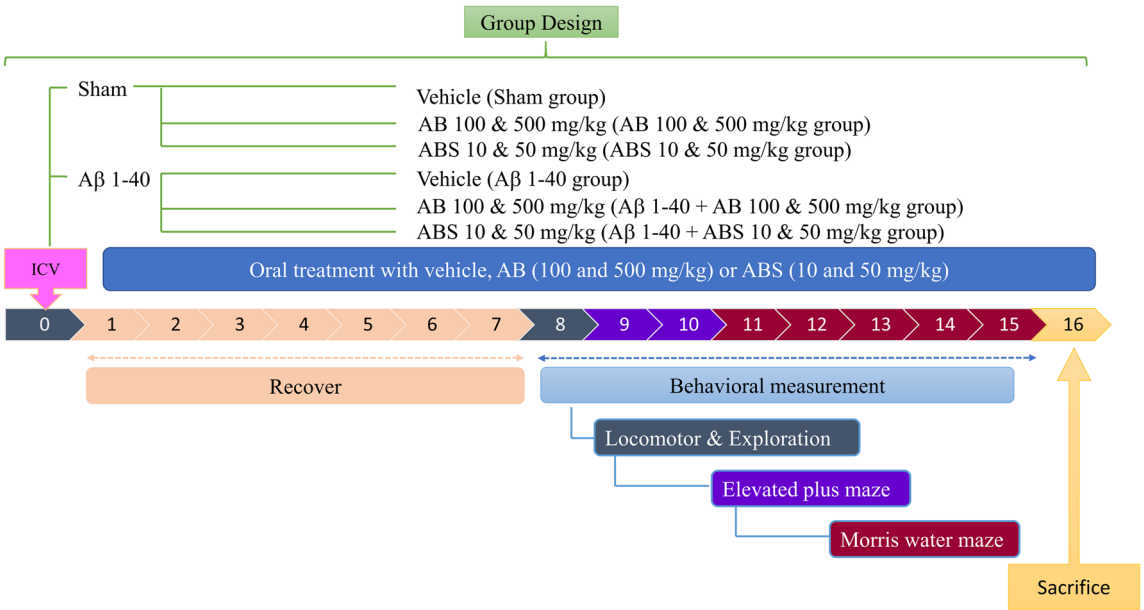

Fig. 1 Experimental design

the central platform, and the transfer latency was measured. After entering the enclosed arm, the animal could move freely in the maze for 10 s and was returned to its home cage. The retention session always followed 24 h after the acquisition session [22]. The transfer latency in the acquisition and retention sessions was recorded using a video camera and an automated video tracking system device equipped with EthoVision XT software (Noldus Information Technology, Leesburg, VA, USA).

Morris Water Maze

The spatial performance test in Morris Water Maze (MWM) was performed on days 11–14 after Aβ 1–40 injection. A black circular stainless pool (with a diameter of 165 cm and a height of 60 cm) was filled with water at 23 ± 1 °C to a 35-cm depth. Each rat underwent four training sessions each day over four consecutive days to find the Plexiglass hidden platform (with a diameter of 10 cm) that was submerged 1.0 cm below the water surface. A trial was initiated by placing the rat in the water facing the pool wall in one of the four quadrants. The daily choice of initial quadrant was randomized, such that all four quadrants were used once each day. For each trial, the rat could swim for a maximum of 120 s to find the platform. When successful, the rat was allowed a 30-s rest period on the platform. If unsuccessful, the rat was given a score of 120 s and then physically placed on the platform and, like a successful rat, given a 30-s rest period. In both cases, each rat was immediately given its next trial. The swim path and escape latency to the platform of a white rat in the black pool were recorded using the above tracking system and EthoVision XT software [21]. On the next day (day 15), the probe test was performed to measure the reference memory. The platform was removed, and each rat was released from the quadrant opposite to where the platform had been located. The parameters included the time spent and distance moved in each quadrant was measured during 60 s [21].

Immunohistochemical Staining Procedure

Rats were anesthetized with pentobarbital (45 mg/kg) and perfused with saline through their left cardiac ventricle, followed by 4% paraformaldehyde in physiological saline. After post-fixation, paraffin brain slices were prepared and cut into sections (10 μm) using a microtome (Leica 2030 Biocut). Some sections were removed paraffin, rehydrated by using conventional histological techniques, and then stained with hematoxylin and eosin. Some sections were incubated with a mouse anti-human amyloid β protein 17–24 monoclonal antibody (Dakopatts A/C; Glostrup, Denmark), a mouse glial fibrillary acidic protein (GFAP) monoclonal antibody (Leica Biosystems Nussloch GmbH; Cambridge, Germany), or a goat anti-IBA-1 polyclonal antibody (Abcam plc; Nuβloch, England), respectively. Immunolabeled sections were developed with 0.05% diaminobenzidine using a Vectastain kit (Vector Laboratories, Burlingame, CA, USA). The modified Gallyas silver impregnation was performed to detect NFT [23]. Brain sections were stained with FD NeuroSilver Kit II (FD NeuroTechnologies, Columbia MD), according to manufacturer instructions. Digital pictures were taken using × 20 or × 40 objectives (Nikon, Tokyo). Results were expressed as the average intensity of the positive immunoreactive cells of GFAP or IBA-1 immunohistochemistry (positive pixels)/the full area captured (total pixels) using the image processing and analysis using Java software (Windows version, National Institutes of Health, Bethesda, MD, USA).

Biochemical Assessments

Preparation of Cortical and Hippocampal Tissues

After behavioral tests, all rats were sacrificed. Their brains were removed and separated into cortex and hippocampus on ice, according to the protocol of Glowinski and Iversen [24]. All brain tissues were homogenized in 9 vol ice-cold PBS. Homogenates were centrifuged at 12,000 rpm for 15 min at 4 °C, and the aliquots of supernatants were separated and stored at − 80 °C until use. The aliquots of supernatants were used to determine AChE activities, antioxidant enzyme activities, and the levels of MDA and GSH.

Estimation of Cortical and Hippocampal AChE Activities

Cortical and hippocampal AChE activity was measured by our previous method [21]. The supernatant solution or AChE standard solution was incubated with 5,5′-dithiobis(2-nitrobenzoic acid) (DTNB) at 25 °C for 10 min, and then 0.3 mM acetylthiocholine iodide was added for color development. The yellow anion of 5-thio-2-nitrobenzoic acid was produced and measured at 412 nm with a spectrophotometric microplate reader. Cortical and hippocampal AChE activity was expressed as U AChE /mg protein.

Estimation of Cortical and Hippocampal Antioxidant Enzyme Activities

The activities of antioxidant enzyme, including for catalase, GPx, GR, and SOD, were measured with a spectrophotometric microplate reader [25]. First, catalase activity was determined with the decrease in the absorbance of amplex red at 560 nm. SOD activity was measured kinetically with the production of nitroblue tetrazolium whose absorbance is at 560 nm. The activities of GPx and GR were measured by Cayman assay kit. SOD and catalase were expressed as U/mg of protein. GPx and GR activities were expressed as mU/mg of protein.

Estimation of Cortical and Hippocampal GSH and MDA Levels

GSH and MDA levels were determined by our previous method [25]. Briefly, the supernatant solution or GSH standard solution was pipetted into each well of a 96-well plate. The reaction solution, included 660 μM DTNB, 900 μM NADPH, and 4.5 U/mL and GR, was added to each well and then recorded at 405 nm for 5 min in a microplate reader. GSH levels were expressed as pmol/mg of protein. The thiobarbituric acid reactive substances (TBARS) assay was used to measure cortical and hippocampal MDA levels. Briefly, the supernatant solution or MDA standard solution was pipetted into 1.5 mL tubes, and a thiobarbituric acid (TBA) test was performed. Next, the absorbance of the above reaction solution was determined at 532 nm. MDA levels were expressed as nmol/mg of protein.

Estimation of Cortical and Hippocampal Cytokine Levels

Cortical and hippocampal tissues were homogenized with protease inhibitor solution (0.4 M NaCl, 0.05% Tween 20, 0.5% bovine serum albumin, 0.1 mM phenylmethylsulfonylfluoride, 0.1 mM benzethonium chloride, 10 mM EDTA, 10 μg/mL aprotinin). Homogenates were centrifuged at 4 °C at 12,000 rpm, aliquoted, and stored at − 80 °C until analysis. IL-1β, IL-6, and TNF-α protein levels were assessed using ELISA kits (R&D Systems, Abingdon, UK) according to the manufacturer protocol. The levels of IL-1β, IL-6, and TNF-α were expressed as pg/mg of protein.

Western Blotting

Cortical and hippocampal tissues were subjected to western blot analyses to determinate the protein levels of ERK pathway and NF-κB signaling. Briefly, cortical and hippocampal tissues were cut into small pieces and homogenized in 9× cold cytoplasmic extraction buffer (20 mM HEPES pH 7.0, 10 mM KCl, 0.5% NP-40) with a tissue grinder. The homogenate was incubated for 10 min and centrifuged at 1500×*g* for 5 min at 4 °C. The supernatant and pellet were separately collected. The supernatant was transferred to a clean pre-chilled tube and centrifuged at 12,000 rpm for 20 min to obtain the cytoplasmic fraction. The pellet was resuspended in ice-cold nuclear extraction buffer (50 mM Tris pH = 8, 150 mM NaCl, 2 mM EDTA, 1% NP-40) and centrifuged at 13,200 rpm for 30 min to obtain the nuclear fraction. The aliquots of cytoplasmic and nuclear supernatants were separated and stored at − 80 °C until use. The protein concentration was quantified using a Bradford protein assay kit (Bio-Rad) and followed by electrophoretic separation through SDS-PAGE. After transferring the protein samples to PVDF membranes, the samples were blocked with 5% non-fat dry milk and 0.1% Tween-20 in Tris-buffered saline at room temperature for 1 h. Then, the membranes were incubated with primary antibodies against ERK, c-Jun N-terminal kinase (JNK), phospho-JNK (p-JNK), p38 mitogen-activated protein kinase (p38), phospho-p38 (p-p38), NF-κB p65 (p65), phospho NF-κB p65 (pp65) (Cell Singnaling Technology, Danvers, MA, USA), and phospho-ERK (p-ERK) (Santa Cruz Biotechnology, Dallas, Texas, USA), overnight at 4 °C and subsequently incubated with horseradish peroxidase-conjugated goat anti-rabbit or goat anti-mouse IgG. The images were scanned using a LAS-4000 mini imaging system (Fujifilm, Kanagawa, Japan), and the optical density data was analyzed using MultiGauge v3.0 software (Fujifilm, Kanagawa, Japan). For the western blot analyses, β-actin (Proteintech, Rosemont, IL, USA) was served as an internal control. Glyceraldehyde 3-phosphate dehydrogenase (GAPDH) (Proteintech, Rosemont, IL, USA) was served as an internal control of cytoplasmic p65 and pp65. Lamin B (Santa Cruz Biotechnology, Dallas, Texas, USA) was served as an internal control of nuclear p65.

Statistical Analyses

All values were expressed as mean ± standard error of the mean (SEM). IBM SPSS version 20.0 (IBM, Chicago, IL, USA) was used to analyze all results with a one-way ANOVA followed by Scheffe's test. P values < 0.05 were significant.

Results

Contents of Oleanolic Acid, Ursolic Acid, and Ecdysterone in ABS

The phytoconstituents of ABS were assayed using HPLC and the chromatograph is shown in Fig. 2. Each gram of ABS contained 135.11 ± 4.28 mg of ecdysterone. There is lack of oleanolic acid and ursolic acid in ABS.

Effects of ABS on Behavioral Function in PBS-Injected or Aβ 1–40-Injected Rats

Effects of ABS on Locomotor Activities and Exploratory Activities in Open-Filed Task in PBS-Injected or Aβ 1–40-Injected Rats

Intracisternal injection with Aβ 1–40 decreased the time spent in the hole and the number of entries into the hole ($P < 0.05$) (Fig. 3a, b), and then decreased the ratio of spent time to entry number ($P < 0.05$) (Fig. 3c). However, intracisternal injection with Aβ 1–40 did not alter the movement time and distance, and velocity in rats (Fig. 4a–c). ABS (only at 50 mg/kg) increased the time spent in the hole and the number of entries

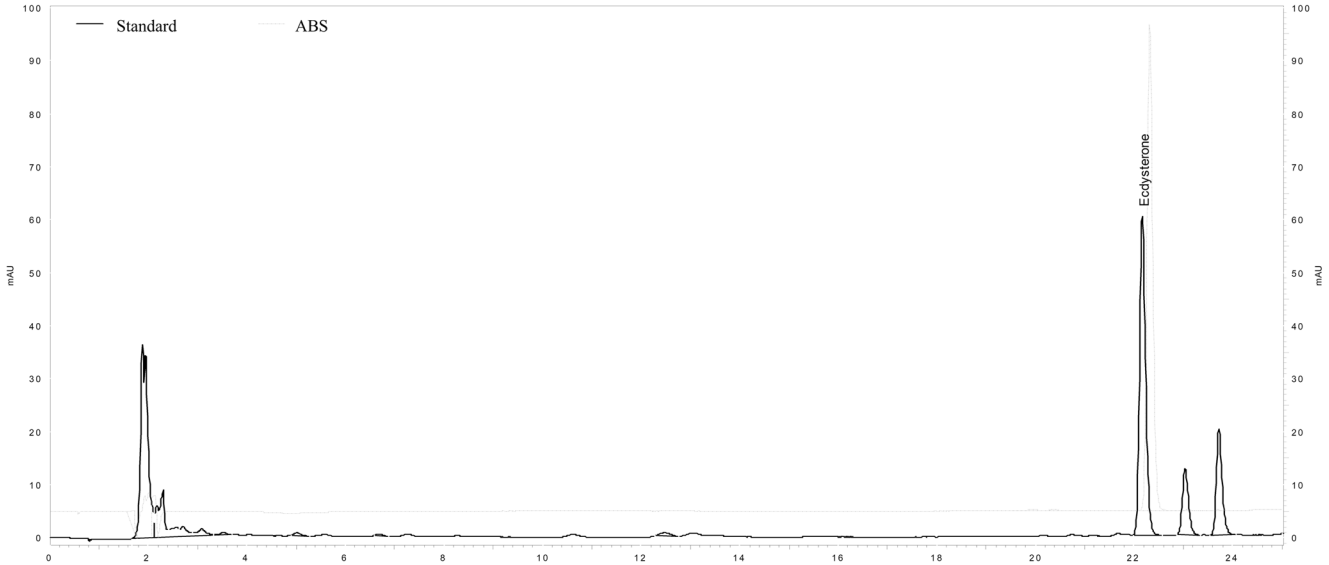

Fig. 2 HPLC chromatograms of steroid-enriched fraction of *Achyranthes bidentata* (ABS, 100 μg/mL) and standard (100 μg/mL) at 280 nm

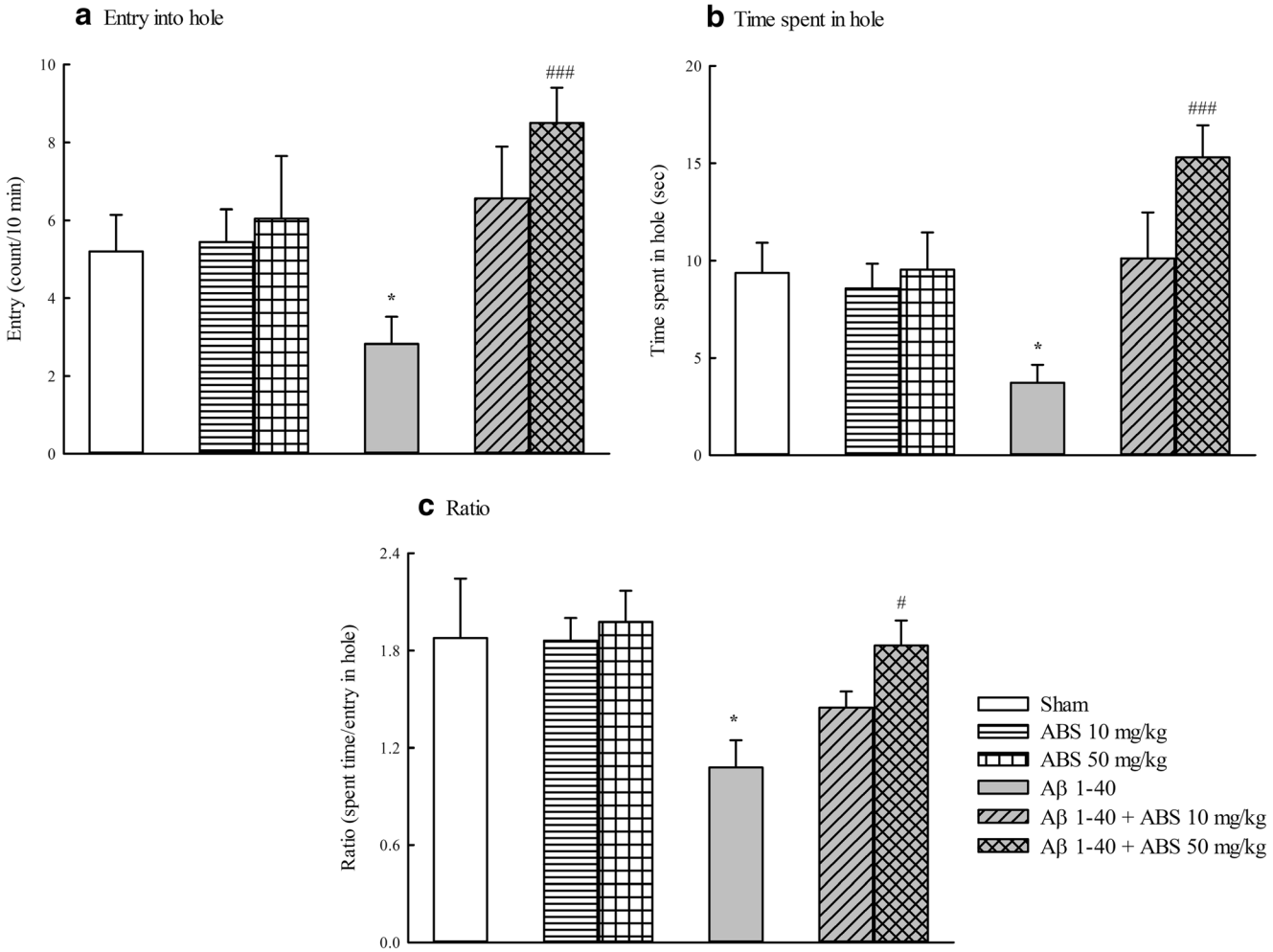

Fig. 3 Effects of steroid-enriched fraction of *Achyranthes bidentata* (ABS, 10 and 50 mg/kg; po) on **a** the number of entries into holes, **b** the time spent in holes, and **c** the ratio in PBS-injected or Aβ 1–40-injected rats. Exploratory test was performed on day 8 after PBS or Aβ 1–40 injection. ABS was continuously administered after PBS or Aβ 1–40 injection until all rats were sacrificed. Columns indicate mean ± SEM ($n = 8$). *$P < 0.05$ as compared to Sham group. #$P < 0.05$, ###$P < 0.001$ as compared to Aβ 1–40-injected group

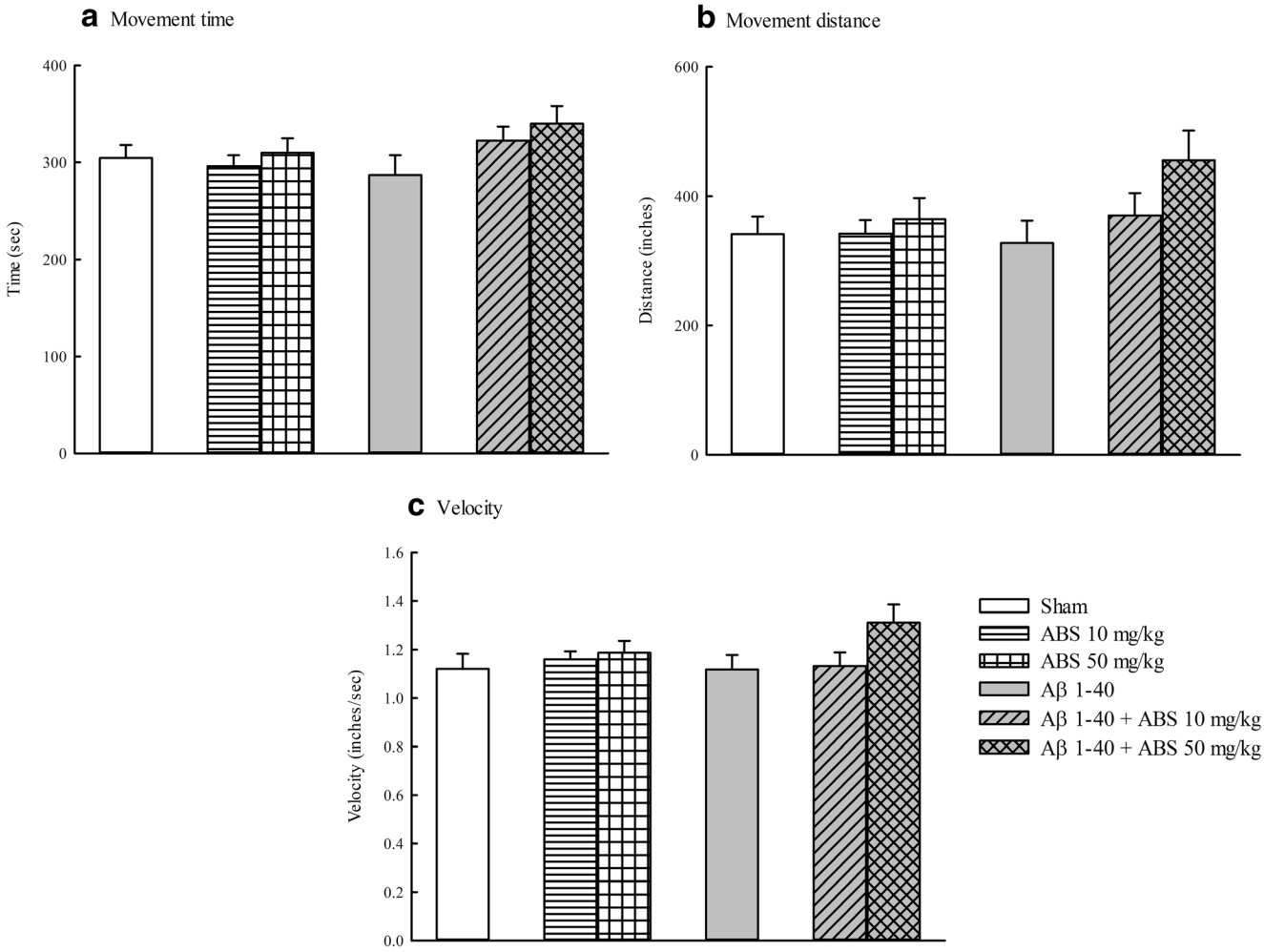

Fig. 4 Effects of steroid-enriched fraction of *Achyranthes bidentata* (ABS, 10 and 50 mg/kg; po) on **a** movement time, **b** movement distance, and **c** velocity in PBS-injected or Aβ 1–40-injected rats. Locomotor test was performed on day 8 after PBS or Aβ 1–40 injection. ABS was continuously administered after PBS or Aβ 1–40 injection until all rats were sacrificed. Columns indicate mean ± SEM ($n = 8$)

into the hole in Aβ 1–40-infused rats ($P < 0.001$) (Fig. 3a, b), and then restored the ratio ($P < 0.05$) (Fig. 3c). ABS at 50 mg/kg also slightly increased the movement activity but not statistical significance in Aβ 1–40-infused rats ($P > 0.05$) (Fig. 4a–c). However, ABS at any dosage did not alter exploratory behavior and motor activity in PBS-injected rats ($P > 0.05$) (Figs. 3 and 4). Furthermore, AB at any dosage did not alter exploratory behavior and motor activity in PBS-injected and Aβ 1–40-infused rats ($P > 0.05$) (Supplementary data—Fig. S1).

Effects of ABS on Spatial Performance and Reference Memory in Elevated Plus-Maze and MWM in PBS-Injected or Aβ 1–40-Injected Rats

Rats intracisternally injected with Aβ 1–40 took a longer transfer latency on retention session (day 2 of elevated plus maze) than sham group ($P < 0.05$) but did not alter transfer latency on acquisition session (day 1 of elevated plus-maze) ($P > 0.05$) (Fig. 5a). Hence, Aβ 1–40 increased the ratio of the transfer latency on retention session to the transfer latency on acquisition session ($P < 0.01$) (Fig. 5b). ABS (only at 50 mg/kg) shortened the longer transfer latency on retention session that was caused by Aβ 1–40 injection and then decreased the ratio ($P < 0.05$) (Fig. 5). Furthermore, ABS at 50 mg/kg also decreased the transfer latency on retention session and the ratio in PBS-injected rats ($P < 0.05$) (Fig. 5). However, AB at any dosage did not alter the ratio of the transfer latency on retention session to the transfer latency on acquisition session in PBS-injected and Aβ 1–40-infused rats ($P > 0.05$) (Supplementary data—Fig. S2(A)).

Rats intracisternally injected with Aβ 1–40 took a longer escape latency on spatial performance test (days 2–4 of MWM) than sham group ($P < 0.01$, $P < 0.001$) (Fig. 6a). Hence, Aβ 1–40 decreased the time spent in the platform area in probe test of MWM than sham group ($P < 0.05$) (Fig. 6b)

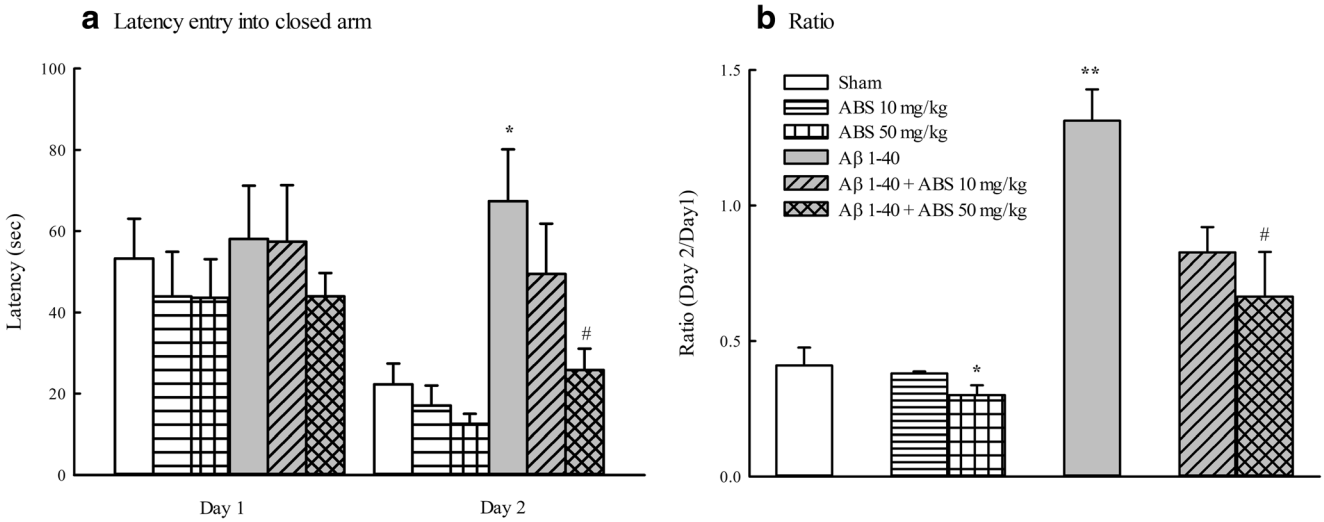

Fig. 5 Effects of steroid-enriched fraction of *Achyranthes bidentata* (ABS, 10 and 50 mg/kg; po) on **a** latency entry into closed arm and **b** the ratio on elevated plus maze in PBS-injected or Aβ 1–40-injected rats. Elevated plus maze was performed on day 9–10 after PBS or Aβ 1–40 injection. ABS was continuously administered after PBS or Aβ 1–40 injection until all rats were sacrificed. Columns indicate mean ± SEM ($n = 8$). *$P < 0.05$; **$P < 0.01$ as compared to Sham group. #$P < 0.05$ as compared to Aβ 1–40-injected group

and mainly increased the percentage spent in outer area (1/3 outer ring of all quadrants of a pool) and decreased the percentage of the platform quadrant in probe test of MWM (Fig. 7). ABS (only at 50 mg/kg) shortened the longer escape latency on spatial performance test (days 2–4 of MWM) that was caused by Aβ 1–40 injection ($P < 0.05$, $P < 0.001$) (Fig. 6a), and then increased the time spent in the platform area and the percentage of the platform quadrant in probe test of MWM ($P < 0.05$) (Figs. 6b and 7). Furthermore, ABS at 50 mg/kg also increased the time spent in the platform area and the percentage of the platform quadrant in probe test of MWM in PBS-injected rats ($P < 0.05$) (Figs. 6b and 7). Finally, any treatment did not alter swimming velocity in the MWM in sham or Aβ 1–40-injected rats ($P > 0.05$) (Fig. 6c). However, AB at any dosage did not alter the escape latency on spatial performance test (day 1–4 of MWM) and the time spent in the platform area in probe test of MWM in PBS-injected and Aβ 1–40-infused rats ($P > 0.05$) (Supplementary data—Fig. S2(B) and (C)).

Effects of ABS on Aβ 1–40 Deposition, Astrocyte, and Microglial Activation

Figure 8a,b presents photographs of immunohistochemical stain of Aβ 1–40 deposition. Aβ 1–40 infusion led to a significant amyloid deposition and NFT in the brain than sham group. ABS at 10 and 50 mg/kg decreased amyloid deposition and NFT in the brain. Figure 8c shows that the neurons in the sham group had normal morphology and clear boundary, while most hippocampal neurons were dark stained or lacking a visible cell boundary in the CA1 areas of Aβ 1–40-injected rats. ABS at 50 mg/kg markedly attenuated the Aβ 1–40-induced neuropathological changes. To clarify the response of astrocyte and microglia, immunohistochemistry staining was used to assess the expression of GFAP (astrocyte activation marker) and IBA-1 (microglia cell activation maker). A significant increase in GFAP-positive staining in the hippocampal CA1 regions from Aβ 1–40-injected rats was found as compared to sham group. The average intensity of GFAP-positive in the CA1 regions from Aβ 1–40-injected rats was increased ($P < 0.001$) (Fig. 8d, f). ABS at 10 and 50 mg/kg decreased GFAP-positive staining and the average intensity of GFAP-positive increased by Aβ 1–40 injection ($P < 0.05$, $P < 0.001$) (Fig. 8d, f). A significant increase in IBA-1-positive staining in the hippocampal CA1 regions from Aβ 1–40-injected rats was also found as compared to sham group. The average intensity of IBA-1-positive in the CA1 regions from Aβ 1–40-injected rats was increased ($P < 0.001$) (Fig. 8e, g). ABS at 10 and 50 mg/kg markedly decreased IBA-1-positive staining and the average intensity of IBA-1-positive increased by Aβ 1–40 injection ($P < 0.05$, $P < 0.001$) (Fig. 8e, g).

Effects of ABS on Cortical and Hippocampal AChE Activities in PBS-Injected or Aβ 1–40-Injected Rats

To clarify the cholinergic mechanism of ABS against Aβ 1–40-injected behavioral deficits in rats, we measured cortical and hippocampal AChE activities. Intracisternal injection with Aβ 1–40 increased cortical and hippocampal AChE activities in rats ($P < 0.001$) (Fig. 9a, b). ABS at 10 and 50 mg/kg prevented cortical and hippocampal AChE activities that was increased by Aβ 1–40 injection ($P < 0.01$, $P < 0.001$)

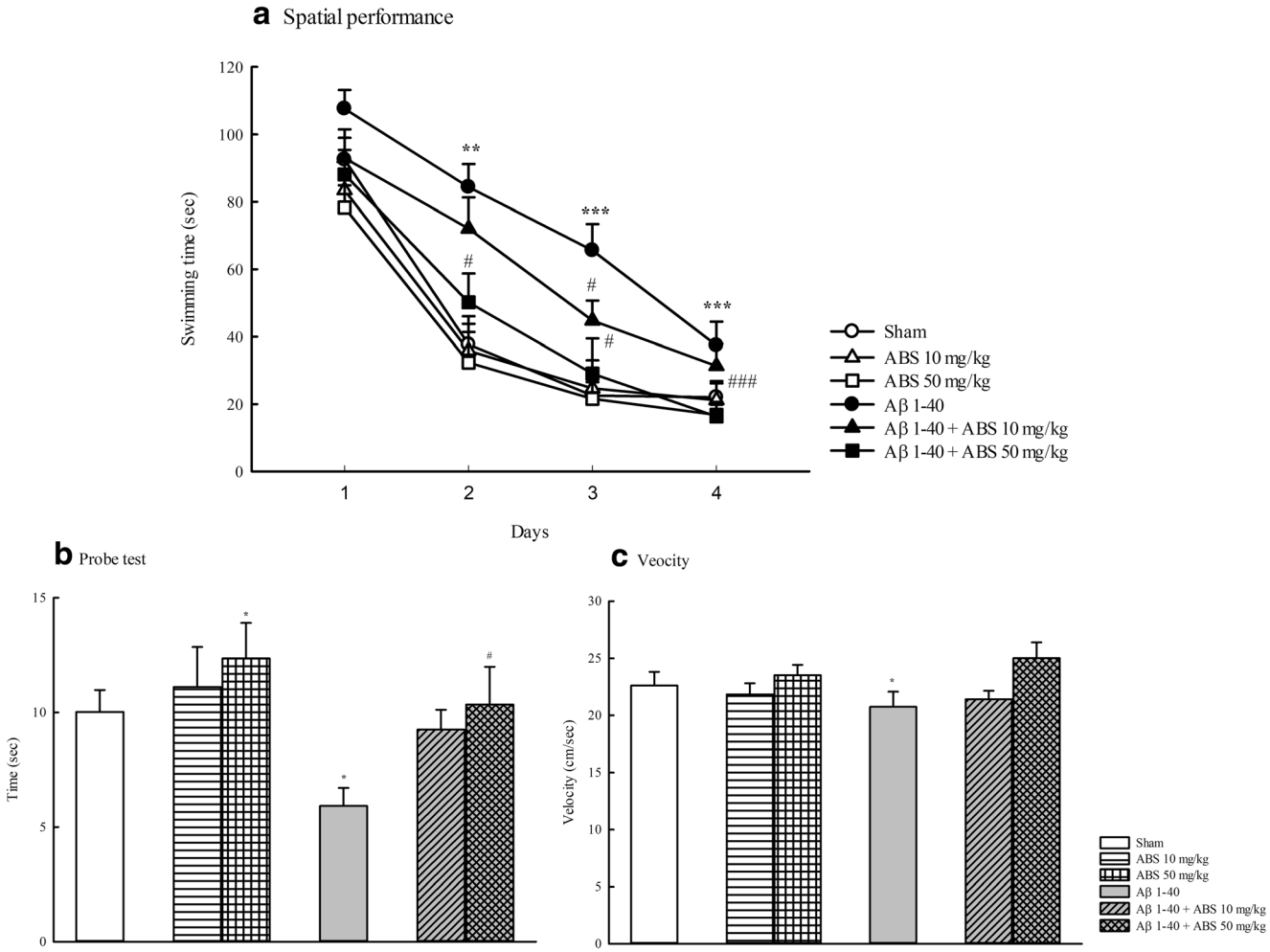

Fig. 6 Effects of steroid-enriched fraction of *Achyranthes bidentata* (ABS, 10 and 50 mg/kg; po) on **a** spatial performance, **b** probe test, and **c** swimming velocity on MWM in PBS-injected or Aβ 1–40-injected rats. Spatial performance and probe test of MWM were performed on days 11–15 after PBS or Aβ 1–40 injection. ABS was continuously administered after PBS or Aβ 1–40 injection until all rats were sacrificed. Columns indicate mean ± SEM ($n = 8$). *$P < 0.05$; **$P < 0.01$; ***$P < 0.001$ as compared to sham group. #$P < 0.05$; ###$P < 0.001$ as compared to Aβ 1–40-injected group

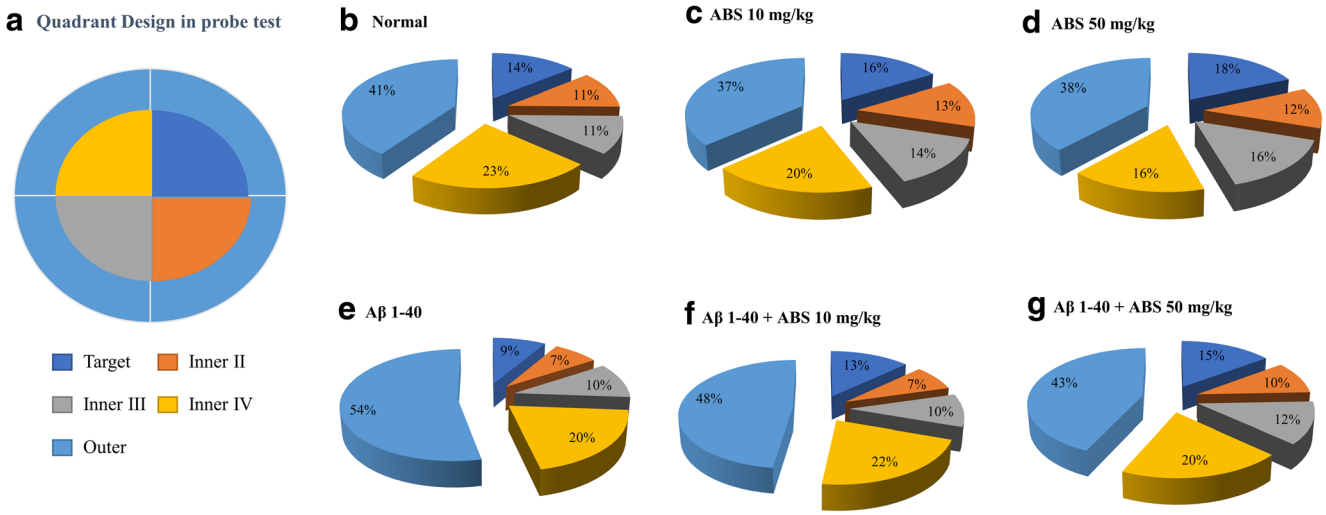

Fig. 7 Effects of steroid-enriched fraction of *Achyranthes bidentata* (ABS, 10 and 50 mg/kg; po) on the probe test of MWM were performed on day 15 after PBS or Aβ 1–40 injection. ABS was continuously administered after PBS or Aβ 1–40 injection until all rats were sacrificed

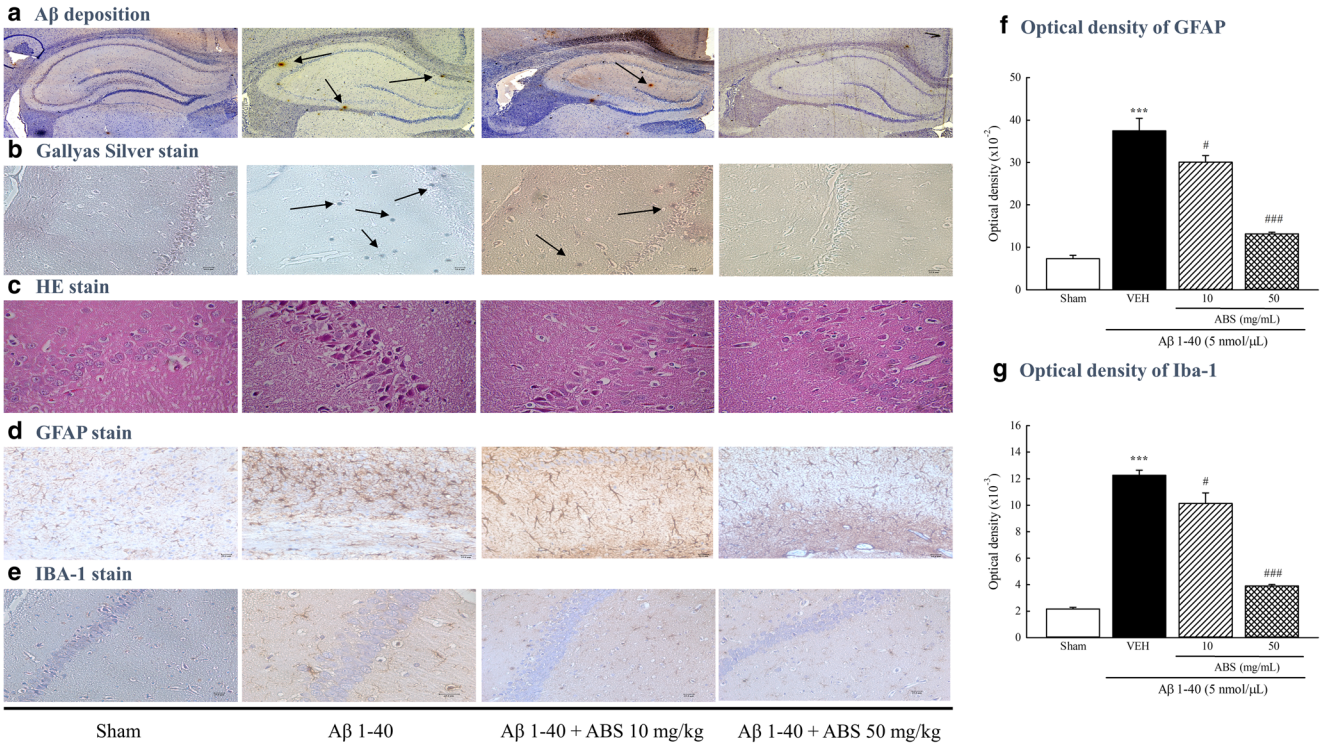

Fig. 8 Effects of steroid-enriched fraction of *Achyranthes bidentata* (ABS, 10 and 50 mg/kg; po) on **a** amyloid deposition, **b** neurofibrillary tangle (Gallyas silver stain), **c** morphological alterations in hippocampus CA1 region, **d** GFAP immunoreactivity of hippocampus CA1 region, **e** IBA-1 immunoreactivity of hippocampus CA1 region, **f** the average optic density of GFAP immunoreactivity, and **g** the average optic density of IBA-1 immunoreactivity. ABS was continuously administered after Aβ 1–40 injection until all rats were sacrificed. Columns indicate mean ± SEM ($n = 4$). ***$P < 0.001$ as compared to Sham group. #$P < 0.05$; ###$P < 0.001$ as compared to Aβ 1–40-injected group

(Fig. 9a, b). However, ABS at any dosage did not alter cortical and hippocampal AChE activities in PBS-injected rats ($P > 0.05$) (Fig. 9a, b).

Effects of ABS on Cortical and Hippocampal Antioxidant Enzymes, Glutathione, and MDA in PBS-Injected or Aβ 1–40-Injected Rats

To clarify the role of antioxidative defense system on the protective effects of ABS against Aβ 1–40-injected behavioral deficits in rats, we measured cortical and hippocampal antioxidant defense system including the levels of GSH, the activities of related antioxidant enzymes, and the levels of oxidative damage maker such as MDA. Intracisternal injection with Aβ 1–40 decreased the activities of cortical and hippocampal antioxidant enzymes including SOD, GPx, GR, and catalase in rats ($P < 0.01$, $P < 0.001$) (Table 1). We further found Aβ 1–40 decreased GSH levels and increased MDA levels in rat cortex and hippocampus ($P < 0.01$, $P < 0.001$) (Fig. 10). ABS at 50 mg/kg restored GSH levels and the activities of antioxidant enzymes in rat cortex and hippocampus that was decreased by Aβ 1–40 injection, and also decreased the higher MDA levels caused by Aβ 1–40 injection ($P < 0.01$, $P < 0.001$) (Table 1; Fig. 10). Furthermore, ABS at 50 mg/kg increased GSH levels and the activities of the antioxidant enzymes in PBS-injected rats ($P < 0.05$, $P < 0.01$, $P < 0.001$) (Fig. 10; Table 1).

Effects of ABS on Cortical and Hippocampal Cytokine Levels in PBS-Injected or Aβ 1–40-Injected Rats

To clarify the anti-inflammatory mechanism on the protective effects of ABS against Aβ 1–40-injected behavioral deficits in rats, we measured the levels of cortical and hippocampal cytokines. Intracisternal injection with Aβ 1–40 increased cortical IL-1β and IL-6 levels in rats ($P < 0.01$) (Fig. 11a, b). We further found Aβ 1–40 increased hippocampal IL-1β, IL-6, and TNF-α levels in rats ($P < 0.01$, $P < 0.001$) (Fig. 11d–f). ABS at 10 and 50 mg/kg decreased IL-1β and IL-6 levels in rat cortex and hippocampus that was increased by Aβ 1–40 injection ($P < 0.05$, $P < 0.01$, $P < 0.001$) (Fig. 11a, b, d–f). However, ABS only at 50 mg/kg decreased hippocampal TNF-α levels that was increased by Aβ 1–40 injection ($P < 0.01$). Furthermore, ABS at 50 mg/kg decreased cortical and hippocampal TNF-α levels in PBS-injected rats ($P < 0.05$) (Fig. 11c, f).

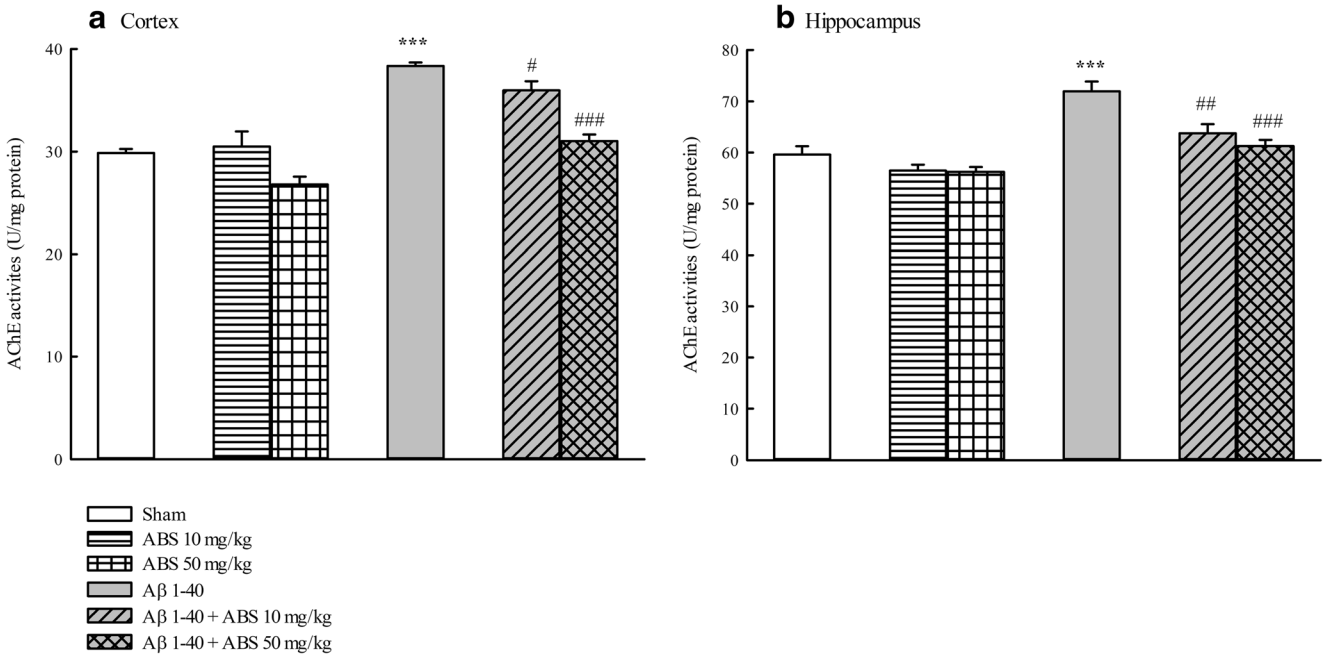

Fig. 9 Effects of steroid-enriched fraction of *Achyranthes bidentata* (ABS, 10 and 50 mg/kg; po) on AChE activities in **a** cortex and **b** hippocampus of PBS-injected or Aβ 1–40-injected rats. ABS was continuously administered after PBS or Aβ 1–40 injection until all rats were sacrificed. Columns indicate mean ± SEM ($n = 8$). ***$P < 0.001$ as compared to sham group. #$P < 0.05$; ##$P < 0.01$; ###$P < 0.001$ as compared to Aβ 1–40-injected group

Effects of ABS on the Protein Expression of Hippocampal ERK Pathway in Aβ 1–40-Injected Rats

To clarify the role of ERK pathway on the protective effects of ABS against Aβ 1–40-injected behavioral deficits in rats, we measured the protein expression of cortical and hippocampal ERK pathway including ERK, JNK, p38, and their phosphorylation. The protein immunoblot assay is shown in Fig. 12a, e. Intracisternal injection with Aβ 1–40 decreased the ratio of *p*-ERK to ERK in cortex and hippocampus ($P < 0.01$, $P < 0.001$) (Fig. 12b, f). However, Aβ 1–40 increased the ratio of *p*-p38 to p38 and the ratio of *p*-JNK to JNK in cortex and hippocampus ($P < 0.01$, $P < 0.001$) (Fig. 12c, d, g–h). ABS at 50 mg/kg restored the ratio of *p*-ERK to ERK, the ratio of *p*-p38 to p38, and the ratio of *p*-JNK to JNK in cortex and hippocampus of Aβ 1–40-infused rats ($P < 0.001$) (Fig. 12b–d, f–h).

Effects of ABS on the Protein Expression and Translocation of Hippocampal NF-κB in Aβ 1–40-Injected Rats

Because neuroinflammation caused by intracisternal injection with Aβ 1–40 mainly is through cytosolic NF-κB p65 phosphorylation and translocation to nucleus, we further assayed the levels of cytosolic NF-κB p65 and NF-κB pp65 protein in the cortex and hippocampus of rat intracisternally injected with Aβ 1–40. The protein immunoblot assay is shown in Fig. 13a, d. Intracisternal injection with Aβ 1–40 increased the ratio of cytosolic pp65 to p65, and also increased the nuclear p65 levels in cortex and hippocampus ($P < 0.01$, $P < 0.001$) (Fig. 13b, c, e, f). ABS at 50 mg/kg decreased the ratio of cytosolic pp65 to p65 and nuclear p65 levels in cortex and hippocampus of Aβ 1–40-infused rats ($P < 0.01$, $P < 0.001$) (Fig. 13b, c, e, f).

Discussion

AB was used as a commonly therapeutic herb for dementia by traditional Chinese physicians. Early report indicated that ethanolic extract of AB inhibited Aβ 1–42 aggregation [14]. According to phytochemical reports, major constituents of AB have been identified as polysaccharides, saponins, and steroids. In the present study, we prepared AB and ABS and demonstrated the anti-dementia potential of AB and ABS in Aβ 1–40-induced AD-like model in rat. Intracisternal injection of Aβ 1–40 produced the deficits of exploratory activities on hole board test and cognitive dysfunction on elevated plus-maze and Morris water maze in rat. Aβ 1–40-injected rats spent more time in the border zone of the pool in comparison to sham group on the probe test of Morris water maze. This behavioral alteration caused by Aβ 1–40 in rats was consistent with our previous report [20]. Together, the above results indicate that the cognitive dysfunction of Aβ 1–40-injected rats in behavioral paradigms is related to the deficit of exploratory behavior and spatial learning impairment. AB at any dosage did not alter behavioral alteration including the dysfunction of

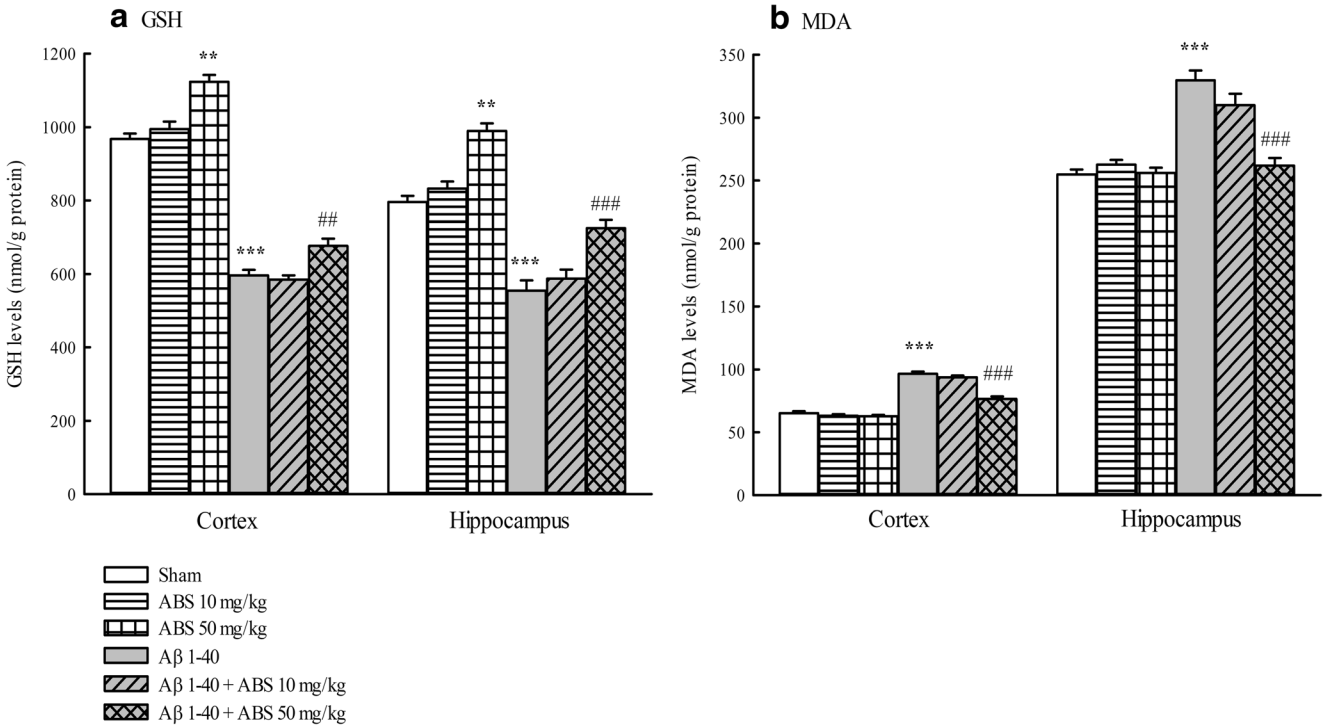

Fig. 10 Effects of steroid-enriched fraction of *Achyranthes bidentata* (ABS, 10 and 50 mg/kg; po) on the levels of **a** GSH and **b** MDA in cortex and hippocampus of PBS-injected or Aβ 1–40-injected rats. ABS was continuously administered after PBS or Aβ 1–40 injection until all rats were sacrificed. Columns indicate mean ± SEM ($n = 8$). $^{**}P < 0.01$; $^{***}P < 0.001$ as compared to Sham group. $^{\#\#}P < 0.01$; $^{\#\#\#}P < 0.001$ as compared to Aβ 1–40-injected group

exploratory activities on hole board test and memory dysfunction on elevated plus-maze and MWM in Aβ 1–40-injected rats. However, ABS (50 mg/kg) improved exploratory activities on hole board test and memory index on elevated plus-maze in Aβ 1–40-injected rats. ABS (50 mg/kg) also improved the spatial performance and reference memory on MWM and took more time in the platform zone of the pool and less time in the border zone of the pool in Aβ 1–40-injected rats, compared to Aβ 1–40-injected group. Therefore, treatment with ABS (steroid-enriched fraction) but not AB (crude extract) improved Aβ 1–40-induced cognitive dysfunction partially via restoring exploratory behavior and promoting memory function in rats. Phytochemical analysis in the present study found ABS only contain ecdysterone (135.11 ± 4.28 mg/g). Ecdysterone is reported to possess neuroprotective effect against neurotoxins Aβ 25–35, MPP^+ and 6-hydroxydopamine in vitro [26–28]. Ecdysterone at 4–8 mg/kg improve the memory dysfunction caused by intrahippocampal injection with Aβ 25–35 [18]. Hence, the major constituent of ABS against Aβ 1–40-induced cognitive dysfunction is ecdysterone (steroids) because the used dosage (50 mg/kg) of ABS, equal to 6.76 mg ecdysterone/kg body weight, is within the range of the memory-improving doses (4–8 mg/kg) of ecdysterone.

According to amyloid cascade hypothesis in the characterized neuropathology of AD, Aβ deposition causes cerebral oxidative stress, NFT, neuroinflammation, and cholinergic neuronal loss [1]. Aβ increased the levels of ROS and elevated oxidative modifications of proteins and lipids such as MDA. The decline in the activities of GSH redox cycle system and antioxidant enzymes such as SOD and catalase has been observed [29]. Then, Aβ deposition and oxidative stress further caused NFT [1, 2]. The present study found intracisternal injection with Aβ 1–40 caused NFT. Intracisternal injection with Aβ 1–40 decreased the activities of antioxidant enzymes including GPx, GR, SOD, and catalase and GSH levels in cortex and hippocampus, and then increased cortical and hippocampal MDA levels. ABS decreased NFT caused by Aβ 1–40 injection. ABS also (50 mg/kg) restored the activities of antioxidant defense system in cortex and hippocampus and decreased cortical and hippocampal oxidative damage. Hence, we suggested that ABS protected Aβ 1–40-induced NFT and neuronal oxidative damage in cortex and hippocampus via activating the activities of antioxidant enzymes including GSH recycle. In addition, neuroinflammation is also an important factor contributing to the progression of AD [29]. Extracellular Aβ depositions have been well documented to play a major role in neuroinflammation [9]. Aggregated Aβ triggers microglia and astrocyte activation, leading to the production of inflammatory factors, including IL-1β, IL-6, and TNF-α, which cause neuronal death

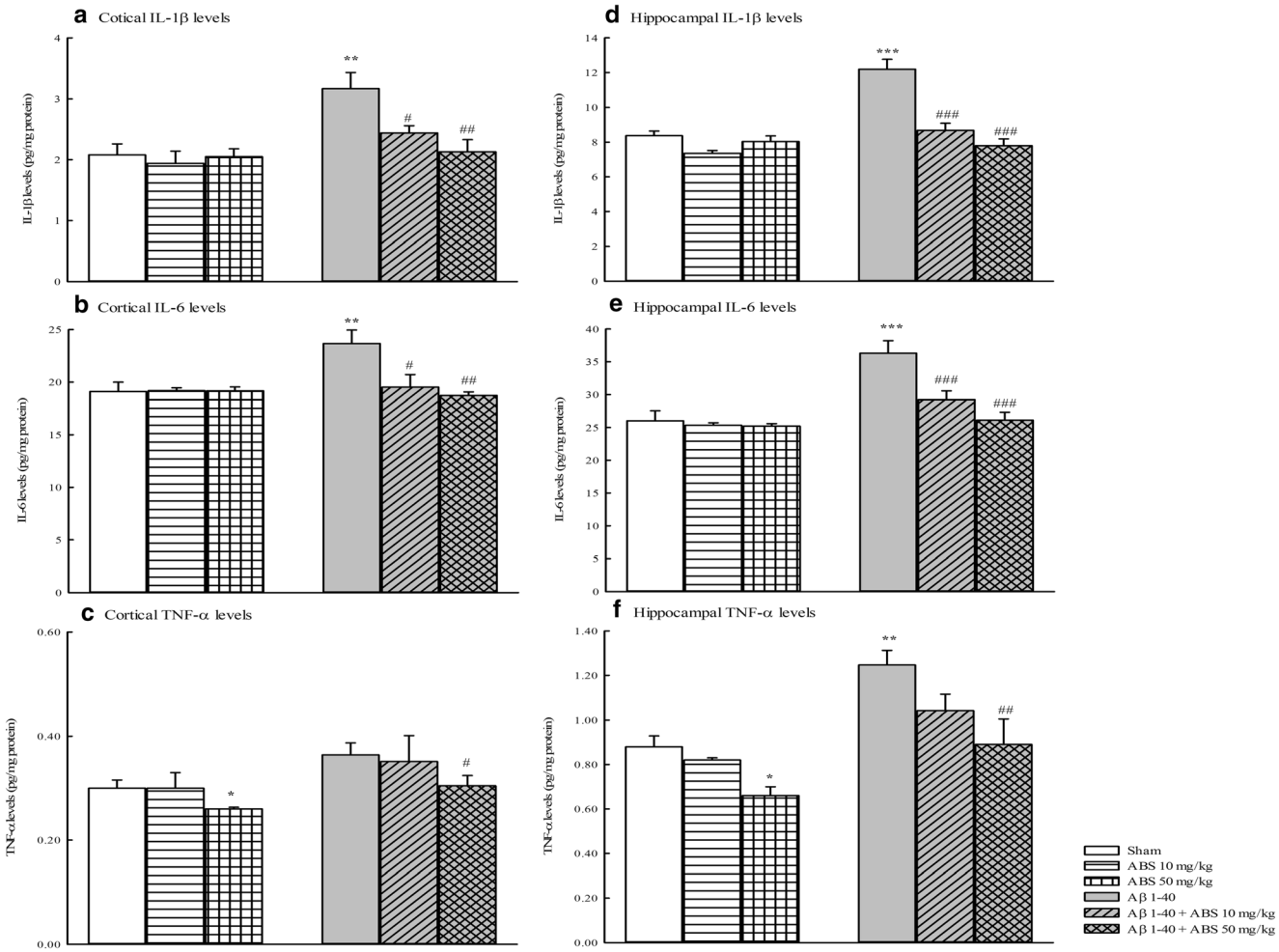

Fig. 11 Effects of steroid-enriched fraction of *Achyranthes bidentata* (ABS, 10 and 50 mg/kg; po) on the cytokine levels in **a**–**c** cortex and d–f hippocampus of PBS-injected or Aβ 1–40-injected rats. **a**, **d** IL-1β. **b**, **e** IL-6. **c**, **f** TNF-α. ABS was continuously administered after PBS or Aβ 1–40 injection until all rats were sacrificed. Columns indicate mean ± SEM ($n = 8$). * $P < 0.05$; ** $P < 0.01$; *** $P < 0.001$ as compared to sham group. #$P < 0.05$; ##$P < 0.01$; ###$P < 0.001$ as compared to Aβ 1–40-injected group

[9, 29]. The present study found intracisternal injection with Aβ 1–40 caused amyloid deposition, microglia, and astrocyte activation, and then increased the levels of cortical and hippocampal cytokines including IL-1β, IL-6, and TNF-α. ABS inhibited amyloid deposition and decreased the neuroinflammatory phenomenon, including microglia and astrocyte activation and elevated cortical and hippocampal cytokines. Furthermore, the present data also indicated that intracisternal injection with Aβ 1–40 caused neuropathological changes and elevated cortical and hippocampal AChE activities. These pathological symptoms were consistent with other reports [6, 21], confirming Aβ 1–40 caused amyloid deposition, oxidative stress, NFT, neuroinflammation, and alteration of cholinergic system (upregulation of AChE activities) in cortex and hippocampus. Aβ 1–40-induced memory deficits are strongly related to a subsequent oxidative stress, NFT, and neuroinflammatory cascade through amyloid deposition that caused central cholinergic dysfunction such as upregulation of AChE activity [29]. ABS (50 mg/kg) also attenuated neuropathological changes and then decreased cortical and hippocampal AChE activities upregulated by Aβ 1–40. Hence, ABS decreased these above neuropathological symptoms caused by Aβ 1–40, confirming that ABS restored cortical and hippocampal cholinergic function through inhibiting amyloid deposition and activating antioxidant defense system and then decreasing oxidative stress, NFT, and neuroinflammation. Early reports have stated that AB protected antimycin A-induced oxidative damage [30] and had anti-inflammatory effects against IL-1β-induced or croton oil-induced inflammation in vitro and in vivo [31, 32]. Its active constituent—ecdysterone—was able to protect MPP^+-induced and H_2O_2-induced oxidative stress in vitro [27, 33]. Ecdysterone also suppressed IL-1β-induced inflammation in vitro [34]. From the present results and the previous reports of AB and its active constituent ecdysterone, ABS and

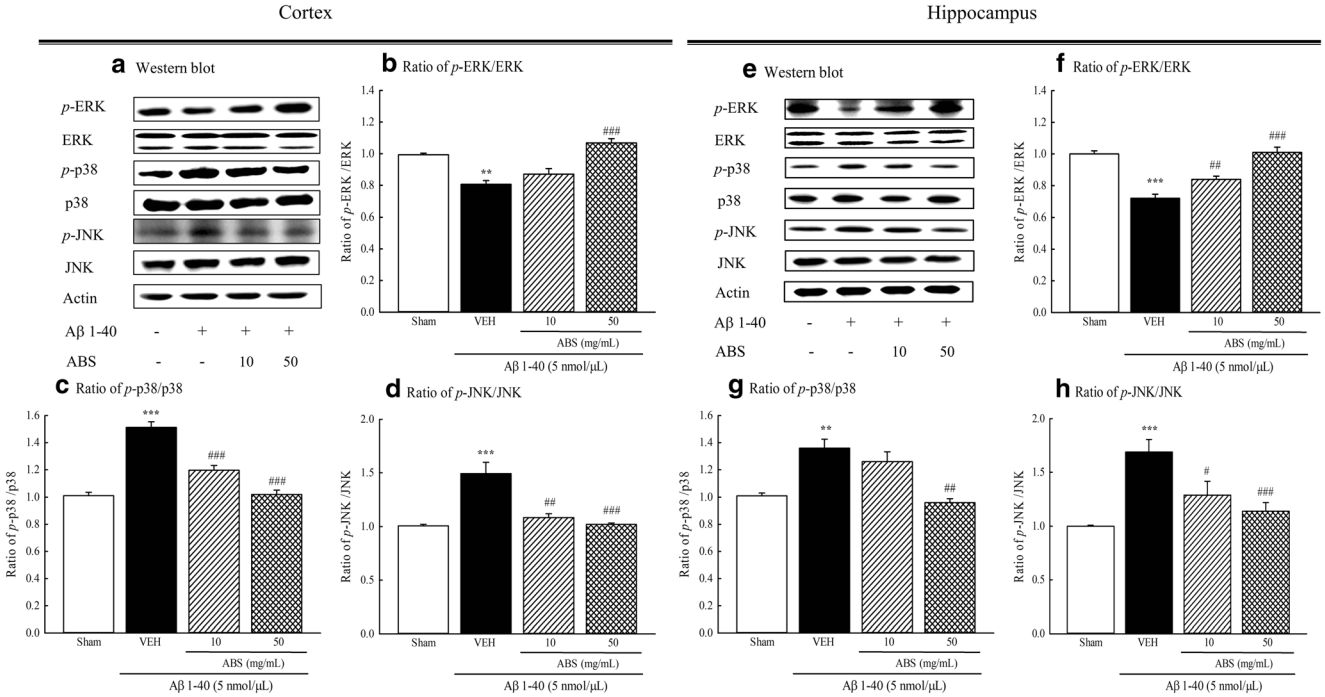

Fig. 12 Effect of steroid-enriched fraction of *Achyranthes bidentata* (ABS, 10 and 50 mg/kg; po) on protein expression of ERK pathway in **a**–**d** cortex and **e**–**h** hippocampus of Aβ 1–40-injected rats. **a**, **e** Protein was determined by immunoblot assay. **b**, **f** Ratio of p-ERK/ERK. **c**, **g** Ratio of p-p38/p38. **d**, **h** Ratio of p-JNK/JNK. ABS was continuously administered after Aβ 1–40 injection until all rats were sacrificed. Columns indicate mean ± SEM ($n = 5$). $^{**}P < 0.01$; $^{***}P < 0.001$ as compared to sham group. $\#P < 0.05$; $\#\#P < 0.01$; $\#\#\#P < 0.001$ as compared to Aβ 1–40-injected group

ecdysterone possess antioxidative and anti-inflammatory activities, hence reduced cortical and hippocampal oxidative stress and neuroinflammation to restore the cholinergic and cognitive function decreased by Aβ 1–40 injection.

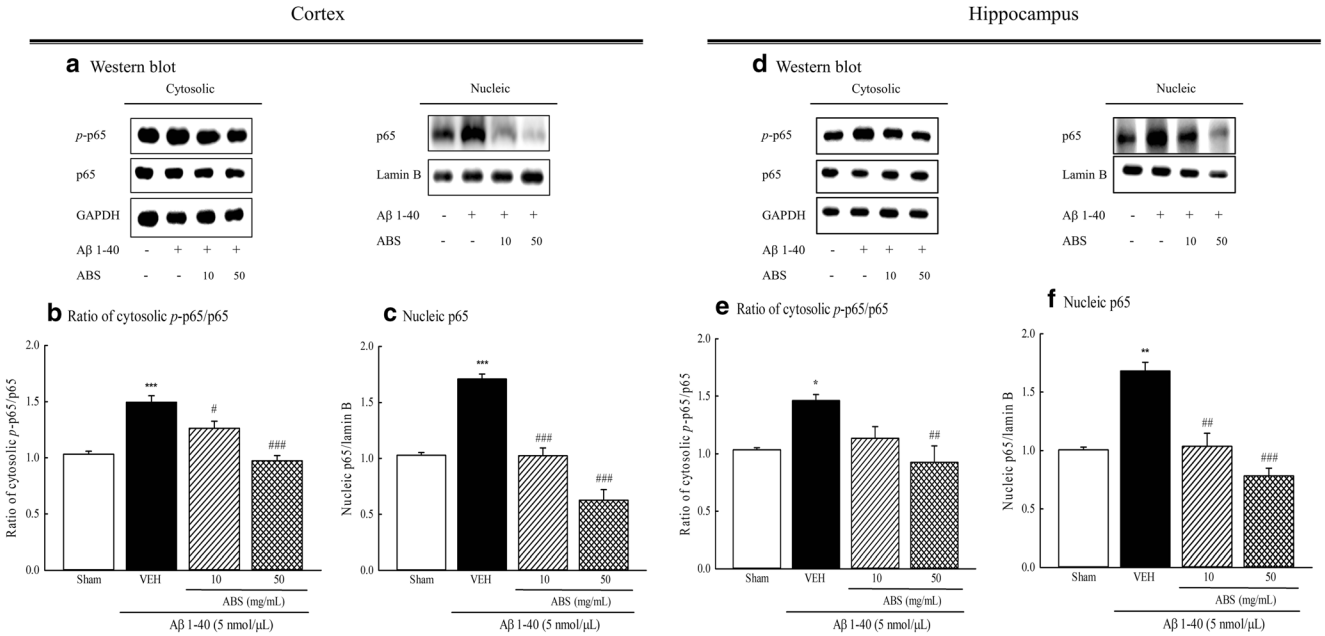

Fig. 13 Effect of steroid-enriched fraction of *Achyranthes bidentata* (ABS, 10 and 50 mg/kg; po) on protein expression and translocation of NF-κB p65 in (**a**–**c**) cortex and (**d**–**f**) hippocampus of Aβ 1–40-injected rats. **a**, **d** Protein was determined by immunoblot assay. **b**, **e** Ratio of cytosolic p-p65/p65. **c**, **f** Nucleic p65. ABS was continuously administered after Aβ 1–40 injection until all rats were sacrificed. Columns indicate mean ± SEM ($n = 5$). $^{*}P < 0.05$; $^{**}P < 0.01$; $^{***}P < 0.001$ as compared to sham group. $\#P < 0.05$; $\#\#P < 0.01$; $\#\#\#P < 0.001$ as compared to Aβ 1–40-injected group

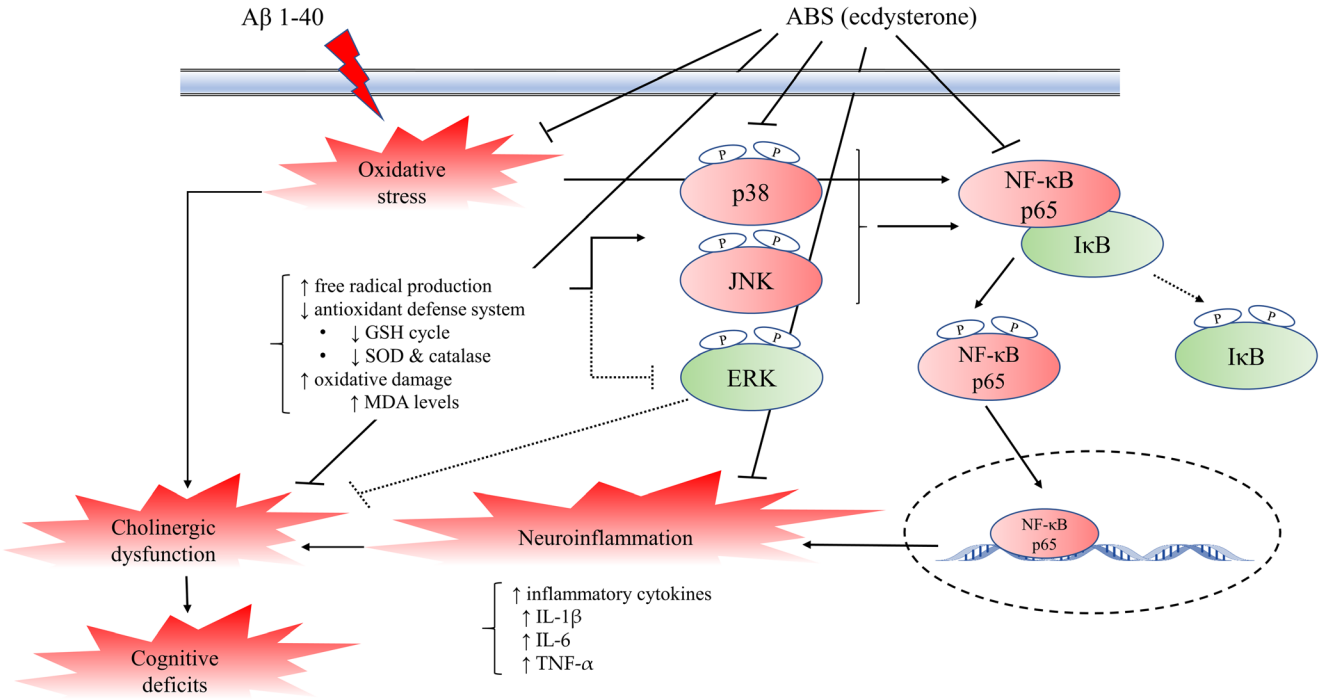

Fig. 14 Schematic representation of the protective mechanism of steroid-enriched fraction of *Achyranthes bidentata* (ABS) in Aβ 1–40-induced AD-like rat model

Increased evidences have certified that many stimuli can activate cytosolic protein kinase members, for instance, MAPK family including three major subfamilies—ERK, JNK, and p38. The present study found that intracisternal injection with Aβ 1–40 promoted the phosphorylation of p38 and JNK in cortex and hippocampus but declined the phosphorylation of ERK. Hence, this present study confirmed the previous reports [35–37] that Aβ 1–40 induced oxidative stress, the inactivation of ERK, and the activation of p38 and JNK, and thus caused neuroinflammation, neuronal damage, and cognitive dysfunction. ABS (50 mg/kg) decreased cortical and hippocampal p38 and JNK phosphorylation upregulated

Table 1 Effects of steroid-enriched fraction of *Achyranthes bidentata* (ABS, 10 and 50 mg/kg, po) on cortical and hippocampal antioxidant enzymes in SD rats intracisternal injected with Aβ 1–40

	The activities of antioxidant enzymes in cortex			
	SOD (U/mg of protein)	GR (mU/mg of protein)	GPx (mU/mg of protein)	Catalase (U/mg of protein)
Sham	271.85 ± 3.38	349.69 ± 5.80	9.50 ± 0.21	62.16 ± 1.90
ABS 10 mg/kg	279.04 ± 6.64	357.65 ± 6.71	10.86 ± 0.28*	65.12 ± 1.75
ABS 50 mg/kg	296.21 ± 9.64*	370.57 ± 4.04*	11.61 ± 0.12**	72.73 ± 1.97***
Aβ 1–40	244.75 ± 3.42***	297.65 ± 5.66***	4.42 ± 0.08***	54.91 ± 1.45**
Aβ 1–40 + ABS 10 mg/kg	245.61 ± 4.05	316.98 ± 5.99	6.56 ± 0.14###	54.76 ± 1.14
Aβ 1–40 + ABS 50 mg/kg	279.71 ± 2.97###	345.47 ± 7.89##	7.77 ± 0.14###	62.93 ± 1.87##
	The activities of antioxidant enzymes in hippocampus			
	SOD (U/mg of protein)	GR (mU/mg of protein)	GPx (U/mg of protein)	Catalase (U/mg of protein)
Sham	170.66 ± 2.94	98.38 ± 1.93	8.62 ± 0.25	28.31 ± 1.00
ABS 10 mg/kg	183.91 ± 5.03	99.48 ± 4.23	9.06 ± 0.18	29.40 ± 2.69
ABS 50 mg/kg	214.68 ± 5.31**	109.62 ± 1.24*	10.13 ± 0.22*	34.69 ± 2.21**
Aβ 1–40	105.93 ± 2.31***	84.97 ± 2.39**	6.89 ± 0.35**	22.35 ± 0.62**
Aβ 1–40 + ABS 10 mg/kg	128.05 ± 2.80#	89.64 ± 1.91	7.48 ± 0.13	22.22 ± 1.24
Aβ 1–40 + ABS 50 mg/kg	165.54 ± 1.42###	97.19 ± 2.59##	8.39 ± 0.39#	27.68 ± 1.17##

Columns indicate means ± SEM ($N = 8$)

*$P < 0.05$; **$P < 0.01$; ***$P < 0.001$ as compared to the Sham group. #$P < 0.05$; ##$P < 0.01$; ###$P < 0.001$ as compared to the Aβ 1–40 group

by Aβ 1–40. ABS (50 mg/kg) also restored cortical and hippocampal ERK phosphorylation downregulated by Aβ 1–40. In earlier study about anti-osteoporosis activity, AB saponins promoted osteogenic differentiation of bone marrow stromal cells through activating ERK signaling pathway [13]. Ecdysterone also promoted wound healing and cell proliferation via activating EGFR-ERK signaling pathway in 3T3L1 fibroblasts [38]. Ecdysterone further played a neuroprotective role against 6-hydroxydopamine-induced apoptosis through the inhibition of ROS-dependent p38 pathway in SH-SY5Y cells [26]. Hence, ABS and ecdysterone improve cognitive dysfunction caused by Aβ 1–40 through multiple pleiotropic effects including antioxidative, anti-inflammatory, and neuroprotective activities via modulating MAPKs signaling pathway.

Furthermore, MAPKs family proteins has been implicated in the mechanism of neuroinflammation through activating several downstream transcription factors such as NF-κB. The activation of MAPK family proteins especial JNK and p38 induce phosphorylation and nuclear translocation of NF-κB p65 subunit. When p65 subunit is translocated into the nucleus, it binds to the specific promoter regions of genes encoding pro-inflammatory cytokines such as IL-1β, IL-6, and TNF-α and regulates their gene expression. Compelling evidence also supported that neurodegeneration in the brain of AD patients is associated with the activation of NF-κB [9]. Aβ accumulation activated the transcription of pro-inflammatory mediators such as cytokines through NF-κB signaling pathway [9]. The present study found intracisternal injection with Aβ 1–40 promoted the phosphorylation of NF-κB p65 and nuclear translocation of NF-κB p65 in cortex and hippocampus. Hence, this present study confirmed the Aβ/ROS/NF-κB pathway in Aβ 1–40-induced AD-like model that Aβ 1–40 caused oxidative damage and activated p38 and JNK signaling pathway, and then induced neuroinflammation via activating the phosphorylation of NF-κB p65 subunit and promoting the nuclear translocation of NF-κB p65 in cortex and hippocampus [39–41]. The neuropathological changes, cholinergic inactivation, and cognitive dysfunction were followed by these processes. ABS (50 mg/kg) decreased the phosphorylation of NF-κB p65 and nuclear translocation of NF-κB p65 upregulated by Aβ 1–40 in cortex and hippocampus. In an earlier study about anti-inflammatory activity, AB saponins prevented IL-1β-induced inflammation and apoptosis by preventing IκB phosphorylation and degradation in rat articular chondrocytes [31]. Ecdysterone also prevented IL-1β-induced inflammation and apoptosis via inhibition of NF-κB signaling pathway in rat articular chondrocytes [34]. Ecdysterone further play a neuroprotective role against H_2O_2-induced oxidative damage through inhibiting the activation of NF-κB in human lens epithelial cells [33]. Hence, ABS and ecdysterone improved cognitive dysfunction caused by Aβ 1–40 through antioxidative and anti-inflammatory activities via modulating MAPKs/NF-κB signaling pathway.

Finally, we found that ABS (steroid-enriched fraction) (50 mg/kg) but not AB (crude extract) promoted the memory index, spatial performance, and reference memory on elevated plus-maze and MWM in PBS-injected rats. This effect is similar to the nootropic effects of *A. aspera* L. as another source of Niu-Xi in traditional Chinese Medicine [42]. Furthermore, ABS (50 mg/kg) activated the activities of antioxidant enzymes and increased GSH levels in cortex and hippocampus of PBS-injected rats. ABS (50 mg/kg) also decreased cortical and hippocampal TNF-α levels in PBS-injected rats. However, ABS at any doses did not alter cortical and hippocampal AChE activities in PBS-injected rats. Hence, ABS (steroid-enriched fraction) alone has the potential to promote cognitive function and regulate brain antioxidant and immune activities. The LD_{50} of AB and ecdysterone is 146.49 g/kg and 6.4 g/kg when intragastric administered to mice [43]. Therefore, we suggest that ABS is an effective and safe fraction of AB because the used dose (50 mg/kg) is within the range of clinical therapeutic doses (5–12 g/day) described in Taiwan Herbal Pharmacopeia or Pharmacopeia of People's Republic of China [16, 17].

In conclusion, the present study raised oxidative stress, neuroinflammation, and their downstream signal system such as ROS/MAPKs/NF-κB pathway might contribute to the neurodegeneration and cognitive dysfunction in Aβ 1–40-induced AD-like rat model. Intracisternal injection with Aβ 1–40 caused cortical and hippocampal oxidative stress and neuroinflammation, and thus promoted p38 and JNK phosphorylation to upregulate NF-κB phosphorylation and translocation. NF-κB translocation increased the expression of proinflammatory cytokines and caused oxidative stress and neuroinflammation again. The vicious cycle among Aβ deposition, oxidative stress, neuroinflammation, and MAPKs/NF-κB pathway caused neuropathological changes (NFT), neuronal loss, cholinergic dysfunction, and cognitive deficits. According to the present results and other reports [13, 14, 30, 31], ABS showed neuroprotective and anti-dementia actions due to its multiple pleiotropic effects including anti-inflammatory, antioxidative, and cellular signaling modulating properties. Then, ecdysterone is an active constituent of ABS from HPLC chromatogram of the present study and also possesses neuroprotective and anti-dementia actions through these above multiple pleiotropic effects from other reports (Fig. 14) [18, 26–28, 33, 34]. Through the verification of the present study, we have confirmed the rationale for clinical use of ABS in dementia or neurodegenerative disorders.

Funding information Financial support is from the Ministry of Science and Technology, Taiwan (NSC 100-2320-B-214 -001, MOST104-2320-B-039-027-MY2, and MOST105-2622-B-039-003-CC2) and ISU-103-01-E-02.

Compliance with ethical standards

The Institutional Animal Care and Use Committee of I-Shou University approved the experimental protocol (IACUC-ISU-9905), and the animals were cared according to the Guiding Principles for the Care and Use of Laboratory Animals.

Abbreviation Aβ, amyloid β peptide; AB, *Achyranthes bidentata*; ABS, steroid-enriched fraction of *Achyranthes bidentata*; AChE, acetylcholinesterase; AD, Alzheimer's disease; DTNB, 5,5′-dithiobis(2-nitrobenzoic acid); ERK, extracellular signal–regulated kinase; GADPH, glyceraldehyde 3-phosphate dehydrogenase; GFAP, glial fibrillary acidic protein; GPx, glutathione peroxidase; GR, glutathione reductase; GSH, glutathione; HPLC, high-performance liquid chromatography; IBA-1, ionized calcium binding adaptor molecule 1; IL-1β, interleukin-1β; IL-6, interleukin-6; JNK, c-Jun N-terminal kinase; MAPKs, mitogen-activated protein kinases; MDA, malondialdehyde; MWM, Morris water maze; NADPH, nicotinamide adenine dinucleotide phosphate; NF-κB, nuclear factor kappa-light-chain-enhancer of activated B cells; NFT, neurofibrillary tangle; *p*-ERK, phospho-ERK; PD, Parkinson's disease; *p*-JNK, phospho-JNK; *p*-p38, phospho-p38; *p*-p65, phospho-p65; ROS, reactive oxygen species; SOD, superoxide dismutase; TBA, thiobarbituric acid; TBARS, thiobarbituric acid reactive substances; TNF-α, tumor necrosis factor alpha.

References

1. Karran E, De Strooper B (2016) The amyloid cascade hypothesis: are we poised for success or failure? J Neurochem 139(Suppl 2): 237–252
2. Karran E, Mercken M, De Strooper B (2011) The amyloid cascade hypothesis for Alzheimer's disease: an appraisal for the development of therapeutics. Nat Rev Drug Discov 10(9):698–712
3. Serrano-Pozo A, Frosch MP, Masliah E, Hyman BT (2011) Neuropathological alterations in Alzheimer disease. Cold Spring Harb Perspect Med 1(1):a006189
4. Querfurth HW, LaFerla FM (2010) Alzheimer's disease. N Engl J Med 362(4):329–344
5. Mhillaj E, Morgese MG, Tucci P, Furiano A, Luongo L, Bove M, Maione S, Cuomo V et al (2018) Celecoxib prevents cognitive impairment and neuroinflammation in soluble amyloid beta-treated rats. Neuroscience 372:58–73
6. Zhang Y, Chen C, Jiang Y, Wang S, Wu X, Wang K (2017) PPARgamma coactivator-1alpha (PGC-1alpha) protects neuroblastoma cells against amyloid-beta (Abeta) induced cell death and neuroinflammation via NF-kappaB pathway. BMC Neurosci 18(1):69
7. Budni J, Feijo DP, Batista-Silva H, Garcez ML, Mina F, Belletini-Santos T, Krasilchik LR, Luz AP et al (2017) Lithium and memantine improve spatial memory impairment and neuroinflammation induced by beta-amyloid 1-42 oligomers in rats. Neurobiol Learn Mem 141:84–92
8. Zhang X, He X, Chen Q, Lu J, Rapposelli S, Pi R (2018) A review on the hybrids of hydroxycinnamic acid as multi-target-directed ligands against Alzheimer's disease. Bioorg Med Chem 26(3): 543–550
9. Seo EJ, Fischer N, Efferth T (2017) Phytochemicals as inhibitors of NF-kappaB for treatment of Alzheimer's disease. Pharmacol Res
10. Lee JK, Kim NJ (2017) Recent advances in the inhibition of p38 MAPK as a potential strategy for the treatment of Alzheimer's disease. Molecules 22(8)
11. He X, Wang X, Fang J, Chang Y, Ning N, Guo H, Huang L, Huang X (2017) The genus Achyranthes: A review on traditional uses, phytochemistry, and pharmacological activities. J Ethnopharmacol 203:260–278
12. Zhang S, Zhang Q, Zhang D, Wang C, Yan C (2018) Anti-osteoporosis activity of a novel *Achyranthes bidentata* polysaccharide via stimulating bone formation. Carbohydr Polym 184:288–298
13. He G, Guo W, Lou Z, Zhang H (2014) *Achyranthes bidentata* saponins promote osteogenic differentiation of bone marrow stromal cells through the ERK MAPK signaling pathway. Cell Biochem Biophys 70(1):467–473
14. Luo H, Gu F, Li X (2003) Inhibiting effect of ethanol extract from *Achyranthes bidentata* on a beta 42 aggregation. J Chin Med Mat 26(6):412–415
15. Peng S, Wang C, Ma J, Jiang K, Jiang Y, Gu X, Sun C (2018) *Achyranthes bidentata* polypeptide protects dopaminergic neurons from apoptosis in Parkinson's disease models both in vitro and in vivo. Br J Pharmacol 175(4):631–643
16. Pharmacopeia of People's Republic of China (2015). China medical science press, Beijing
17. Chang YS (2018). Achyranthis bidentatae radix. In: Chen SC (ed) Taiwan Herbal Pharmacopeia. 3rd Edn. Ministry of health and welfare, Taipei, pp 73–74.
18. Yang SF, Yang ZQ, Zhou QX, Wu Q, Huang XN, Shi JS (2004) Effect of ecdysterone on the expression of c-fos in the brain of rats induced by microinjection beta-AP25-35 into the hippocampus. Acta Pharm Sin 39(4):241–244
19. Zhang MM, Zhao HQ, Zhou SD, Wang DJ, Wang X, Liu DC, Geng YL, Mu DJ (2015) Content determination of β-ecdysterone and oleanolic acid in *Achyranthes bidentata Blume* by HPLC and their fingerprints. ShanDong Sci 28(5):1–6
20. Tsai FS, Cheng HY, Hsieh MT, Wu CR, Lin YC, Peng WH (2010) The ameliorating effects of luteolin on beta-amyloid-induced impairment of water maze performance and passive avoidance in rats. Am J Chin Med 38(2):279–291
21. Shiao YJ, Su MH, Lin HC, Wu CR (2017) Echinacoside ameliorates the memory impairment and cholinergic deficit induced by amyloid beta peptides via the inhibition of amyloid deposition and toxicology. Food Funct 8(6):2283–2294
22. Da Cunha IC, Jose RF, Orlandi Pereira L, Pimenta JA, Oliveira de Souza IA, Reiser R, Moreno H Jr, Marino Neto J et al (2005) The role of nitric oxide in the emotional learning of rats in the plus-maze. Physiol Behav 84(3):351–358
23. Uchihara T (2007) Silver diagnosis in neuropathology: principles, practice and revised interpretation. Acta Neuropathol 113(5):483–499
24. Glowinski J, Iversen LL (1966) Regional studies of catecholamines in the rat brain. I. The disposition of [3H]norepinephrine, [3H]dopamine and [3H]dopa in various regions of the brain. J Neurochem 13(8):655–669
25. Kuo HC, Chang HC, Lan WC, Tsai FH, Liao JC, Wu CR (2014) Protective effects of *Drynaria fortunei* against 6-hydroxydopamine-induced oxidative damage in B35 cells via the PI3K/AKT pathway. Food Funct 5(8):1956–1965
26. Pan Z, Niu Y, Liang Y, Zhang X, Dong M (2016) beta-Ecdysterone protects SH-SY5Y cells against 6-hydroxydopamine-induced apoptosis via mitochondria-dependent mechanism: involvement of p38(MAPK)-p53 signaling pathway. Neurotox Res 30(3):453–466
27. Zou Y, Wang R, Guo H, Dong M (2015) Phytoestrogen beta-ecdysterone protects PC12 cells against MPP^+-induced neurotoxicity in vitro: involvement of PI3K-Nrf2-regulated pathway. Toxicol Sci 147(1):28–38

28. Yang SF, Wu ZJ, Yang ZQ, Wu Q, Gong QH, Zhou QX, Shi JS (2005) Protective effect of ecdysterone on PC12 cells cytotoxicity induced by beta-amyloid25-35. Chin J Integr Med 11(4):293–296
29. Kumar K, Kumar A, Keegan RM, Deshmukh R (2018) Recent advances in the neurobiology and neuropharmacology of Alzheimer's disease. Biomed Pharmacother 98:297–307
30. Suh KS, Lee YS, Choi EM (2014) The protective effects of *Achyranthes bidentata* root extract on the antimycin A induced damage of osteoblastic MC3T3-E1 cells. Cytotechnology 66(6): 925–935
31. Xu XX, Zhang XH, Diao Y, Huang YX (2017) *Achyranthes bidentate* saponins protect rat articular chondrocytes against interleukin-1beta-induced inflammation and apoptosis in vitro. Kaohsiung J Med Sci 33(2):62–68
32. Lu T, Mao C, Zhang L, Xu W (1997) The research on analgestic and anti-inflammatory action of different processed products of *Achyranthes bidentata*. J Chin Med Mat 20(10):507–509
33. Feng CY, Huang XR, Qi MX (2012) Effects of ecdysterone on the expression of NF-kappaB p65 in H_2O_2 induced oxidative damage of human lens epithelial cells. Chin J Integr Med 32(1):76–79
34. Zhang X, Xu X, Xu T, Qin S (2014) Beta-ecdysterone suppresses interleukin-1beta-induced apoptosis and inflammation in rat chondrocytes via inhibition of NF-kappaB signaling pathway. Drug Dev Res 75(3):195–201
35. Faucher P, Mons N, Micheau J, Louis C, Beracochea DJ (2015) Hippocampal injections of oligomeric amyloid beta-peptide (1-42) induce selective working memory deficits and long-lasting alterations of ERK signaling pathway. Front Aging Neurosci 7:245
36. Fan CD, Li Y, Fu XT, Wu QJ, Hou YJ, Yang MF, Sun JY, Fu XY et al (2017) Reversal of beta-amyloid-induced neurotoxicity in PC12 cells by curcumin, the important role of ROS-mediated signaling and ERK pathway. Cell Mol Neurobiol 37(2):211–222
37. Li J, Ding X, Zhang R, Jiang W, Sun X, Xia Z, Wang X, Wu E et al (2015) Harpagoside ameliorates the amyloid-beta-induced cognitive impairment in rats via up-regulating BDNF expression and MAPK/PI3K pathways. Neuroscience 303:103–114
38. Omanakuttan A, Bose C, Pandurangan N, Kumar GB, Banerji A, Nair BG (2016) Nitric oxide and ERK mediates regulation of cellular processes by Ecdysterone. Exp Cell Res 346(2):167–175
39. Liu H, Deng Y, Gao J, Liu Y, Li W, Shi J, Gong Q (2015) Sodium hydrosulfide attenuates beta-amyloid-induced cognitive deficits and neuroinflammation via modulation of MAPK/NF-kappaB pathway in rats. Curr Alzheimer Res 12(7):673–683
40. Kim TI, Lee YK, Park SG, Choi IS, Ban JO, Park HK, Nam SY, Yun YW et al (2009) l-Theanine, an amino acid in green tea, attenuates beta-amyloid-induced cognitive dysfunction and neurotoxicity: reduction in oxidative damage and inactivation of ERK/p38 kinase and NF-kappaB pathways. Free Radic Biol Med 47(11): 1601–1610
41. Song YS, Park HJ, Kim SY, Lee SH, Yoo HS, Lee HS, Lee MK, Oh KW et al (2004) Protective role of Bcl-2 on beta-amyloid-induced cell death of differentiated PC12 cells: reduction of NF-kappaB and p38 MAP kinase activation. Neurosci Res 49(1):69–80
42. Gawande DY, Goel RK (2015) Pharmacological validation of in-silico guided novel nootropic potential of *Achyranthes aspera* L. J Ethnopharmacol 175:324–334
43. Li M (2015) Achyranthes bidentata Bl. In: Liu Y, Wang Z, Zhang J (ed) Dietary Chinese herbs chemistry. Pharmacol Clin Evid. 1st edn. Springer, Vienna, 45–52.